Article

Chemical Behavior of the Biradicaloid (HO···ONO) Singlet States of Peroxynitrous Acid. The Oxidation of Hydrocarbons, Sulfides, and Selenides

Robert D. Bach, Olga Dmitrenko, and Carlos M. Estvez

J. Am. Chem. Soc., **2005**, 127 (9), 3140-3155• DOI: 10.1021/ja044245d • Publication Date (Web): 11 February 2005

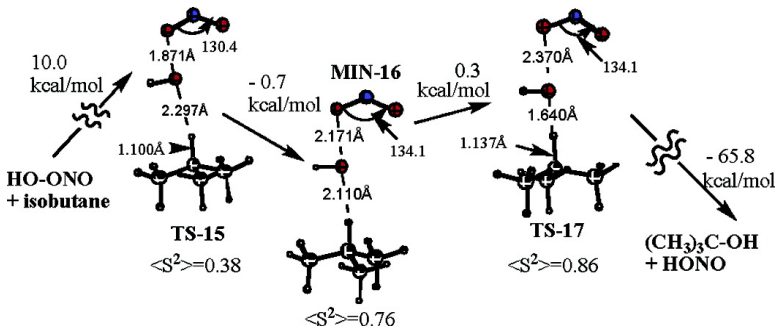

More About This Article

Additional resources and features associated with this article are available within the HTML version:

- Supporting Information
- Links to the 3 articles that cite this article, as of the time of this article download
- Access to high resolution figures
- Links to articles and content related to this article
- Copyright permission to reproduce figures and/or text from this article

View the Full Text HTML

J|A|C|S
ARTICLES
Published on Web 02/11/2005

Chemical Behavior of the Biradicaloid (HO···ONO) Singlet States of Peroxynitrous Acid. The Oxidation of Hydrocarbons, Sulfides, and Selenides

Robert D. Bach,*,† Olga Dmitrenko,† and Carlos M. Estévez‡

Contribution from the Department of Chemistry and Biochemistry, University of Delaware, Newark, Delaware 19716, and Departamento de Química Física, Facultade de Química, Universidade de Vigo, 36200 Spain

Received September 21, 2004; E-mail: rbach@udel.edu

Abstract: Various high levels of theory have been applied to the characterization of two higher lying biradicaloid metastable singlet states of peroxynitrous acid. A singlet minimum (*cis*-**2**) was located that had an elongated O−O distance (2.17 Å) and was only 12.2 kcal/mol [UB3LYP/6-311+G(3df,2p)+ZPVE] higher in energy than its ground-state precursor. A *trans*-metastable singlet (*trans*-**2**) was 10.9 kcal/mol higher in energy than ground-state HO−ONO. CASSCF(12,10)/6-311+G(d,p) calculations predict the optimized geometries of these *cis*- and *trans*-metastable singlets to be close to those obtained with DFT. Optimization of *cis*- and *trans*-**2** within the COSMO solvent model suggests that both exist as energy minima in polar media. Both *cis*- and *trans*-**2** exist as hydrogen bonded complexes with several water molecules. These collective data suggest that solvated forms of *cis*-**2**·3H_2O and *trans*-**2**·3H_2O represent the elusive higher lying biradicaloid minima that were recently (*J. Am. Chem. Soc.* **2003**, *125*, 16204) advocated as the metastable forms of peroxynitrous acid (HOONO*). The involvement of metastable *trans*-**2** in the gas phase oxidation of methane and isobutane is firmly established to take place on the unrestricted [UB3LYP/6-311+G(d,p)] potential energy surface (PES) with classical activations barriers for the hydrogen abstraction step that are 15.7 and 5.9 kcal/mol lower than the corresponding activation energies for producing products methanol and *tert*-butyl alcohol formed on the restricted PES. The oxidation of dimethyl sulfide and dimethyl selenide, two-electron oxidations, proceeds by an S_N2-like attack of the heteroatom lone pair on the O−O bond of ground-state peroxynitrous acid. No involvement of metastable forms of HO−ONO was discernible.

1. Introduction

More than a decade has passed since the physiological significance of peroxynitrous acid (HO−ONO), a fleeting intermediate with a half-life of less than a second, was disclosed by Beckman et al.[1] The peroxynitrite anion (NO−OO^-), formed by the direct combination of nitric oxide (NO) and superoxide anion (O_2^-) is stable in alkaline solution. At physiological pH, the anion is partially protonated and its fate in aqueous media has been a primary point of contention. It was suggested that this strong oxidant might be a source of very potent biologically relevant hydroxyl radicals.[2] One of the more intriguing aspects of HO−ONO chemistry is the earlier suggestion that O−O bond homolysis was slow and the reactive species is a vibrationally excited form of HOONO.[2d] However, its lifetime of $\sim 10^{-11}$ s would preclude its involvement in bimolecular reactions, and Pryor et al.[3] advocated the existence of a high-energy metastable form of peroxynitrous acid (HO−ONO*) that is in steady-state equilibrium with ground-state HO−ONO. A number of theoretical groups have unsuccessfully attempted to characterize such a metastable form of HO−ONO. Consequently, conventional wisdom has proposed either homolysis to produce •OH and •NO_2 or a caged radical (•OH···•NO_2). Careful experimentation has suggested that the yield of hydroxyl radicals at room temperature in deoxygenated and bicarbonate free water at pH 6.8 is about 10%.[4] However, reports of the yields of hydroxyl radicals from the decomposition of HO−ONO have ranged from 0 to 40%.[4a] To date no experimental evidence has been presented for the presence of such a metastable species. There have also been numerous experimental and theoretical studies on the potential role peroxynitrous acid plays in three-body recombination reactions involving OH and NO_2 in atmospheric chemistry.[5]

There have been several theoretical studies that have described the geometry,[6a] decomposition pathways[6b] and reactivity[7a,b,8a] of peroxynitrous acid. The ground-state (GS) structures of HO−

† University of Delaware.
‡ Universidade de Vigo.

(1) Beckman J. S.; Beckman, T. W.; Chen, J.; Marshall, P. A.; Freeman, B A. *Proc. Natl. Acad. Sci. U.S.A.* **1990**, *87*, 1620.
(2) (a) Pryor, W. A. *Am. J. Physiol.* **1995**, *268*, L699. (b) Pryor, W. A.; Jin, X.; Squadrito, G. L. *Proc. Natl. Acad. Sci. U.S.A.* **1994**, *91*, 11173. (c) Koppenol, W. H.; Moreno, J. J.; Pryor, W. A.; Ischiropoulos, H.; Beckman, J. S. *Chem. Res. Toxicol.* **1992**, *5*, 834. (d) Crow, J. P.; Spruell, C.; Chen, J.; Gunn, C.; Ischiropoulos, H.; Tsai, M.; Smith, C. D.; Radi, R.; Koppenol, W. H.; Beckman, J. S. *Free Radical Biol. Med.* **1994**, *16*, 331.
(3) Pryor, W. A.; Jim, X.; Squadrito, G. L. *J. Am. Chem. Soc.* **1996**, *118*, 3125.
(4) (a) Richeson, C. E.; Mulder, P.; Bowry, V. W.; Ingold, K. U. *J. Am. Chem. Soc.* **1998**, *120*, 7211. (b) Hodges, G. R.; Ingold, K. U. *J. Am. Chem. Soc.* **1999**, *121*, 10695.
(5) Mathews, J.; Sinha, A.; Francisco, J. S. *J. Chem. Phys.* **2004**, *120*, 10543.

10.1021/ja044245d CCC: $30.25

ONO have been well studied by a number of theoretical groups.[6−8] A thermally excited form of peroxynitrous acid (HO−ONO*) has only recently been located by maintaining the search for an optimized geometry minimum on the unrestricted or open-shell surface. In a preliminary report we described cis and trans higher lying singlet minima of peroxynitrous acid (HO···ONO) at several levels of theory including CASSCF.[9] We now expand upon this new development and also provide theoretical data that these metastable forms of peroxynitrous acid (HO−ONO*) are directly implicated in the gas-phase oxidation of methane and isobutane to methanol and *tert*-butanol but do not appear to be involved in the oxidation of dimethyl sulfide or dimethyl selenide.

2. Computational Details

Quantum chemistry calculations were carried out using the Gaussian98 program[10a] system utilizing gradient geometry optimization.[10d−f] Geometries were fully optimized using the B3LYP functional[11] with 6-311+G(d,p), 6-311+G(3df,2p), and Aug-cc-pVTZ basis sets. Vibrational frequency and IRC calculations at the same level as the geometry optimization were performed to characterize the stationary points as either minima or transition structures (first-order saddle point). Corrections for solvation were made using polarizable conductor COSMO model calculations.[12a] Multireference complete active space (CASSCF) calculations were performed mostly with the GAMESS[13] program. For the multireference configuration interaction (MRCI) calculations and CIPT2 correlation corrections to the CASSCF wave function, the MOLPRO[14] suite of programs was used. The Gaussian03[10b] program was employed for examination of the effect of basis set superposition error (BSSE) using the counterpoise method. The refinement of the relative energies of metastable states *cis*-**2** and *trans*-**2** and hydrogen bonded structures **4A** and **4B** utilized a variation of the G3B3 scheme in Gaussian03[10c] where we used geometry optimization and scaled zero-point vibrational energy corrections, ZPVE, (scale factor 0.96) at the B3LYP/6-311+G(3df,2p) level instead of the standard protocol at B3LYP/6-31G(d). The general expression for the total G3B3 energy has not been changed from its original form.[10c]

$$E_0(\mathrm{G3}) = E[\mathrm{MP4(FC)/6\text{-}31G(d)}] + \Delta(+) + \Delta(\mathrm{2df,p}) + \Delta(\mathrm{QCI}) + \mathrm{HLC} + \mathrm{ZPVE}$$

where

$$\Delta(+) = E[\mathrm{MP4(FC)/6\text{-}31{+}G(d)} - \mathrm{MP4(FC)/6\text{-}31G(d)}]$$

$$\Delta(\mathrm{2df,p}) = E[\mathrm{MP4(FC)/6\text{-}31G(2df,p)} - \mathrm{MP4(FC)/6\text{-}31G(d)}]$$

$$\Delta(\mathrm{QCI}) = E[\mathrm{QCISD(T,FC)/6\text{-}31G(d)} - \mathrm{MP4(FC)/6\text{-}31G(d)}]$$

$$\mathrm{HLC} = -6.760n_\beta - 3.233(n_\alpha - n_\beta)$$

the n_α and n_β are the number of α and β valence electrons ($n_\alpha \geq n_\beta$),

All the calculations on the "excited" HO···ONO stationary points indicate a significant triplet spin contamination in the wave function, as evidenced by the $\langle S^2\rangle$ values close to 1. Therefore, the nature of the wave functions for these structures is intermediate between singlet and triplet spin multiplicities, and the energy values so obtained need to be refined by a spin-projection method to eliminate the spin contaminants. This was accomplished in an approximate way by using the formula suggested by Yamaguchi et al.[12b−d] It allows elimination of the triplet contaminant of the singlet:

$$E_{sc} = E_{mix} + f_{sc}(E_{mix} - E_{triplet})$$

E_{sc} and E_{mix} denote the spin corrected and noncorrected (obtained using guess = mix) singlet energies; $E_{triplet}$ is a triplet energy (single-point calculation). The fraction of spin contamination, f_{sc}, was calculated according to the formula:

$$f_{sc} = \langle S^2\rangle_{mix}/(\langle S^2\rangle_{triplet} - \langle S^2\rangle_{mix})$$

3. Results and Discussion

(a) Characterization of the Elusive Higher Lying Singlet States of Peroxynitrous Acid. While the GS *cis* conformer is the ground state for HO−ONO at B3LYP, the perpendicular conformer is slightly more stable at the QCISD and CASSCF levels (Figure 1A).

We initiated our study with a search for the so-called "excited state" that would presumably have a highly elongated O−O bond. A potential problem associated with the location of such a biradicaloid species on the unrestricted potential energy surface (PES) is that, despite attempting to optimize with an unrestricted (UB3LYP) description, the wave function can converge to the restricted solution ($\langle S^2\rangle = 0$). However, you can be assured of at least starting the geometry search with an unrestricted initial guess by mixing HOMO and LUMO (guess = mix,

(6) (a) Sumathi, R.; Peyerimhoff, S. D. *J. Chem. Phys.* **1997**, *107*, 1872. (b) Dixon, D. A.; Feller, D.; Zhan, C. G.; Francisco, J. S. *J. Phys. Chem. A* **2002**, *106*, 3191.
(7) (a) Shustov, G. V.; Spinney, R.; Rauk, A. *J. Am. Chem. Soc.* **2000**, *122*, 1191. (b) Olson, L. P.; Bartberger, M. D.; Houk, K. N. *J. Am. Chem. Soc.* **2003**, *125*, 3999. (c) Houk, K. N.; Condroski, K. R.; Pryor, W. A. *J. Am. Chem. Soc.* **1996**, *118*, 13002. (d) Rudakov, E. S.; Lobachev, V. L.; Geletii, Y. V. *Chem. Res. Toxicol.* **2001**, *14*, 1232. (e) Shustov, G. V.; Rauk, A. *J. Org Chem.* **1998**, *63*, 5413.
(8) (a) Bach, R. D.; Glukhovtsev, M. N.; Canepa, C. *J. Am. Chem. Soc.* **1998**, *120*, 775. (b) Bach, R. D.; Ayala, P. Y.; Schlegel, H. B. *J. Am. Chem. Soc.* **1996**, *118*, 12758. (c) Bach, R. D.; McDouall, J. J. W.; Owensby, A. L.; Schlegel, H. B. *J. Am. Chem. Soc.* **1990**, *112*, 7064. (d) Bach, R. D.; Owensby, A. L.; Gonzalez, C. Schlegel, H. B.; McDouall, J. J. W. *J. Am. Chem. Soc.* **1991**, *113*, 6001.
(9) Bach, R. D.; Dmitrenko, O.; Estevez, C. M. *J. Am. Chem. Soc.* **2003**, *125*, 16204.
(10) (a) Frisch, M. J.; Trucks, G. W.; Schlegel, H. B.; Scuseria, G. E.; Robb, M. A.; Cheeseman, J. R.; Zakrzewski, V. G.; Montgomery, J. A.; Stratmann, R. E.; Burant, J. C.; Dapprich, S.; Millam, J. M.; Daniels, A. D.; Kudin, K. N.; Strain, M. C.; Farkas, O.; Tomasi, J.; Barone, V.; Cossi, M.; Cammi, R.; Mennucci, B.; Pomelli, C.; Adamo, C.; Clifford, S.; Ochterski, J.; Petersson, G. A.; Ayala, P. Y.; Cui, Q.; Morokuma, K.; Malick, D. K.; Rabuck, A. D.; Raghavachari, K.; Foresman, J. B.; Cioslowski, J.; Ortiz, J. V.; Baboul, A. G.; Stefanov, B. B.; Liu, G.; Liashenko, A.; Piskorz, P.; Komaromi, I.; Gomperts, R.; Martin, R. L.; Fox, D. J.; Keith, T.; Al-Laham, M. A.; Peng, C. Y.; Nanayakkara, A.; Gonzalez, C.; Challacombe, M.; Gill, P. M. W.; Johnson, B.; Chen, W.; Wong, M. W.; Andres, J. L.; Gonzalez, C.; Head-Gordon, M.; Replogle, E. S.; Pople, J. A. *Gaussian 98*, revision A.7; Gaussian, Inc.: Pittsburgh, PA, 1998. (b) *Gaussian 03*, revision B.05 (SGI64-G03RevB.05); Gaussian, Inc.: Pittsburgh, PA, 2003. (c) Baboul, A. G.; Curtiss, L. A.; Redfern, P. C.; Raghavachari, K. *J. Chem. Phys.* **1999**, *110*, 7650. (d) Schlegel, H. B. *J. Comput. Chem.* **1982**, *3*, 214. (e) Schlegel, H. B. *Adv. Chem. Phys.* **1987**, *67 (Pt. 1)*, 249. (f) Schlegel, H. B. In *Modern Electronic Structure Theory*; Yarkony, D. R., Ed.; World Scientific: Singapore, 1995; p 459.
(11) (a) Becke, A. D. *Phys. Rev. A* **1988**, *38*, 3098. (b) Lee, C.; Yang, W.; Parr, R. G. *Phys. Rev. B* **1988**, *37*, 785. (b) Becke, A. D. *J. Chem. Phys.* **1993**, *98*, 5648. (b) Stevens, P. J.; Devlin, F. J.; Chabalowski, C. F.; Frisch, M. J. *J. Phys. Chem.* **1994**, *98*, 11623.
(12) (a) Barone, V.; Cossi, M.; Tomasi, J. *J. Comput. Chem.* **1998**, *19*, 404. (b) Yamaguchi, K.; Jensen, F.; Dorigo, A.; Houk, K. N. *Chem. Phys. Lett.* **1988**, *149*, 537. (c) Yamanaka, S.; Kawakami, T.; Nagao, K.; Yamaguchi, K. *Chem. Phys. Lett.* **1994**, *231*, 25. (d) Wittbrodt, J. M.; Schlegel, H. B. *J. Chem. Phys.* **1996**, *105*, 6574.
(13) The GAMESS (General atomic and molecular electronic structure system) program: Schmidt, M. W.; Baldridge, K. K.; Boatz, J. A.; Elbert, S. T.; Gordon, M. S.; Jensen, J. H.; Koseki, S.; Matsunaga, N.; Nguyen, K. A.; Su, S.; Windus, T. L.; Dupuis, M.; Montgomery, J. A., Jr. *J. Comput. Chem.* **1993**, *14*, 1347. (c) Fletcher, G. D.; Schmidt, M. W.; Gordon, M. S. *Adv. Chem. Phys.* **1999**, *110*, 267.
(14) MOLPRO is a package of ab initio programs designed by H.-J. Werner and P. J. Knowles. The authors are R. D. Amos, A. Bernhardsson, A. Berning, P. Celani, D. L. Cooper, M. J. O. Deegan, A. J. Dobbyn, F. Eckert, C. Hampel, G. Hetzer, P. J. Knowles, T. Korona, R. Lindh, A. W. Lloyd, S. J. McNicholas, F. R. Manby, W. Meyer, M. E. Mura, A. Nicklass, P. Palmieri, R. Pitzer, G. Rauhut, M. Schütz, U. Schumann, H. Stoll, A. J. Stone R. Tarroni, T. Thorsteinsson, and H.-J. Werner.

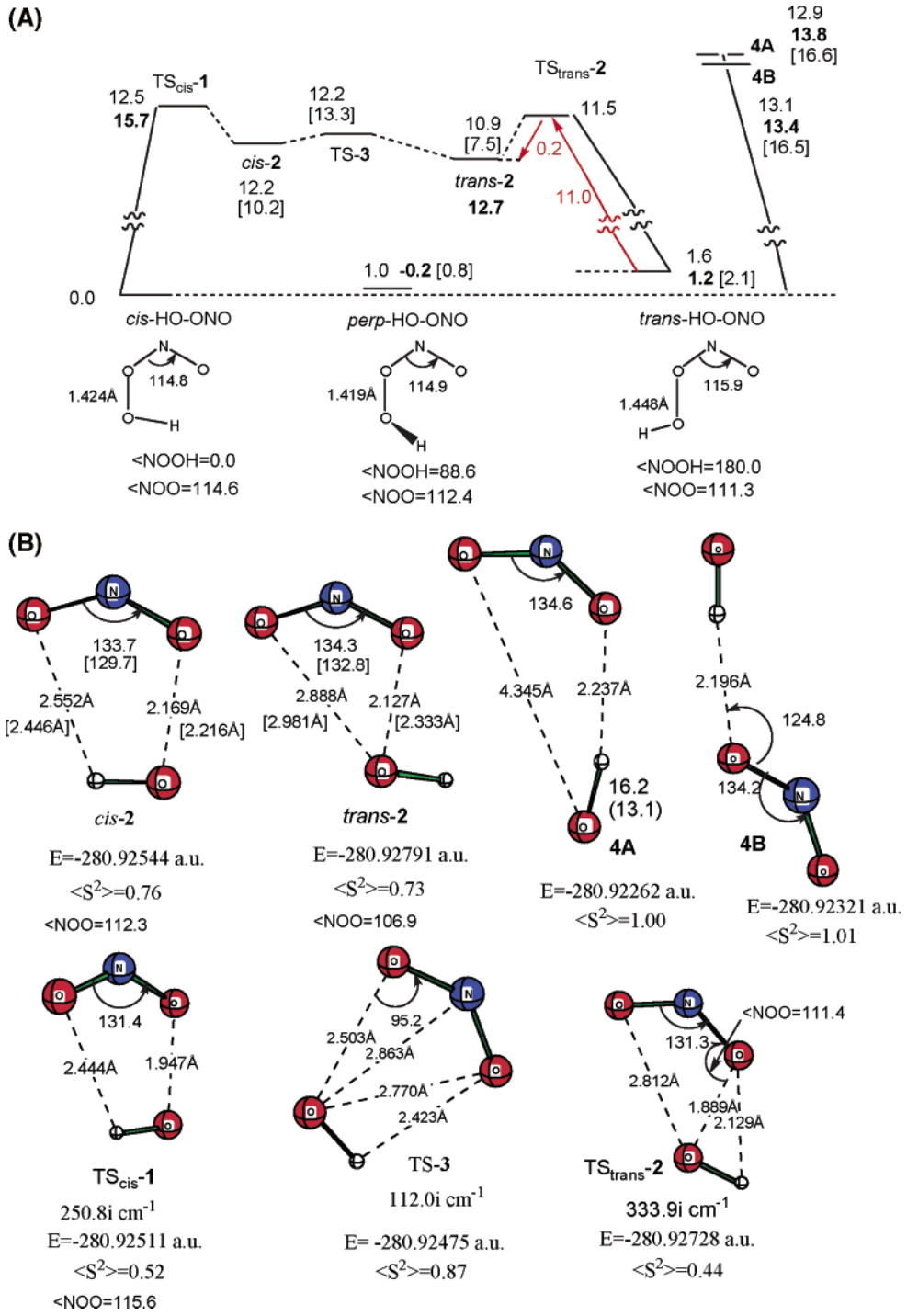

Figure 1. (A) Energy diagram showing the relative energies of metastable HO−ONO isomers and their transition structures (TS$_{cis}$-**1** and TS$_{trans}$-**2**) for O−O bond elongation of ground state *cis*- and *trans*-HO−ONO to form their respective higher lying singlet biradicaloid minima *cis*-**2** and *trans*-**2**. Structures **4A** and **4B** are isomers of *cis*-**2** and *trans*-**2** with the OH radical hydrogen bonded to the $^2A_1$ state of NO_2 radical. Plain numbers are at the UB3LYP/6-311+G-(3df,2p) +ZPVE level. Numbers in brackets are spin-corrected G3B3//UB3LYP/6-311+G(3df,2p) relative energies. Bold numbers correspond to UQCISD-(T)/6-311+G(d,p)//UQCISD/6-311+G(d,p). Red numbers are B3LYP//B3LYP/Aug-cc-pVTZ energy differences between trans-HO−ONO and TS$_{trans}$-**2** and between trans-**2** and TS$_{trans}$-**2**. For a summary of the calculations at other levels of theory, see Table 1. (B) UB3LYP/6-311+G(3df,2p)-optimized biradicaloid minima and transition structures characterized on the energy diagram. Geometrical data in brackets are at the CAS(12,10)/6-311+G(d,p) level.

$\langle S^2 \rangle = 1.0$).[10a] Following this protocol, using a fairly flexible basis set [6-311+G(d,p) or larger] with a relatively small step size, we were able to readily locate a singlet minimum (A′ symmetry) having an elongated O−O distance of 2.17 Å that was only 12.2 kcal/mol [UB3LYP/6-311+G(3df,2p) + ZPVE] higher in energy than its *cis*-peroxynitrous acid GS precursor (Figure 1, *cis*-**2**). A second higher lying minimum, *trans*-**2**, derived from the *trans*-conformer of HO−ONO was only 10.9 kcal/mol higher in energy than ground-state HO−ONO. At the UQCISD(T)//UQCISD/6-311+G(d,p) level, *trans*-**2** is 12.7 kcal/mol higher in energy than GS *cis*-HO−ONO in excellent agreement with the DFT calculations. The ONO fragments of

Table 1. Relative Energies (kcal/mol) for HOONO and Its Isomeric Compounds Calculated at Different Levels of Theory[a]

	A	B	C	D	E	F	G	S–T
cis-HO−ONO	0.0	0.0	0.0	0.0	0.0		0.0	
perp-HO−ONO	1.4 (1.0)	1.4 (1.0)	−0.2 (1.2)	0.7	0.8	0.0	−0.4 *−0.9*	
trans-HO−ONO	2.6 (1.6)	2.6 (1.9)	1.2 (2.5)	2.1	2.1			
TS_{cis}-**1**	14.6 (12.5)	7.8 (5.7)	15.7 (6.3)	19.1	3.9		(15.9)	17.2 (19.3)
	0.52		**0.98**					
cis − **2**	14.4 (12.2)	8.2 (5.8)	(13.4)	18.0	10.2	11.7	12.7 (15.1)	8.0 (10.0)
	12.1 **0.77**		**1.02**				**1.04**	
							11.4 (14.3)	
TS-**3**	14.8 (12.2)	10.6 (8.0)	(15.8)	16.8	13.3			3.7 (5.4)
	0.87		**1.03**					
trans − **2**	12.9 (10.9)	6.7 (4.6)	12.7 (11.3)	17.3	7.5	9.0 (4.9)	11.1 (13.6)	10.4 (10.8)
	10.8 **0.73**		**1.00**				**1.01**	
							12.3 (12.1)	
TS_{trans} -**2**	13.2 (11.5)	7.2 (5.4)	(1.3)	17.9	0.4		10.0 (14.0)	20.0 (21.7)
	0.43		**0.96**				**0.98**	
4A	16.2 (12.9)	16.3 (13.0)	13.8 (18.9)	16.6	16.6			0.1 (−0.1)
	14.9 **1.01**		**1.04**					
4B	15.8 (13.1)	15.8 (13.1)	13.4 (18.5)	16.5	16.5		(13.2) **1.05**	0.2 (0.0)
	14.6 **1.01**		**1.03**					

[a] **A**: UB3LYP/6-311+G(3df,2p) (without ZPVE). Numbers in parenthesis are with ZPVE; numbers in italic are calculated at the same level with Gaussian 03 solvent correction, COSMO (solvent = water); the $\langle S^2 \rangle$ values are given in bold. **B**: spin corrected UB3LYP/6-311+G(3df,2p). Numbers in parentheses are with ZPVE. **C**: [UQCISD(T)/6-311+G(d,p)//UQCISD/6-311+G(d,p). Numbers in parentheses are at the spin corrected UQCISD(T,E4T)/6-31G(d)//UB3LYP/6-311+G(3df,2p) level; the $\langle S^2 \rangle$ values are given in bold. **D**: G3B3//B3LYP/6-311+G(3df,2p). **E**: Spin corrected G3B3//B3LYP/6-311+G(3df,2p). **F**: MRCI and CIPT2 (in parentheses) relative energies with correlation correction applied to the CAS(12,10)/6-311+G(d,p) results. **G**: RBD(TQ)//UB3LYP/6-311+G(3df,2p). Numbers in parentheses are at the UBD(TQ)//UB3LYP/6-311+G(3df,2p) level obtained with guess = mix; the resulting $\langle S^2 \rangle$ values are given in bold; numbers in italic correspond to the same restricted and unrestricted BDTQ calculations on CAS(12,10)/6-311+G(d,p)-optimized structures. The last column contains singlet−triplet energy gaps without spin correction (S−T, kcal/mol) at the G3B3 and UB3LYP/6-311+G(3df,2p) (in parenthesis) levels of theory for UB3LYP/6-311+G(3df,2p) optimized structures.

the metastable states appear to correlate with the $^2A_1$ state of the NO_2 radical with an ONO bond angle of ∼134° as discussed below.

The transition state for O−O bond stretching (TS_{cis}-**1**, R_{O-O} = 1.947 Å, ν = 250.8i cm^{-1}) was found to be only 0.3 kcal/mol higher in energy than metastable singlet *cis*-**2**. The TS associated with formation of slightly more stable singlet *trans*-**2** (Figure 1A) was 11.5 kcal/mol above the GS cis minimum for HO−ONO (TS_{trans}-**1**, R_{O-O} = 1.889 Å, ν = 333.9i cm^{-1}). Both of these TSs have reaction vectors comprised largely of O−O bond elongation with secondary contributions from expansion of the ONO angle to its $^2A_1$ state with an ONO bond angle of ∼134°. While both TSs have a contribution from hydrogen bonding of the O−H hydrogen with the proximal oxygen of the developing ONO fragment, neither TS upon animation of the vectors looks like it is connected to H-bonding complexes **4A** and **4B**. The expansion of the O····H−O angle approaching the ∼180° in **4A** and **4B** is absent from both TSs prompting us to suggest that TS_{cis}-**1** and TS_{trans}-**2** are connected to metastable isomers *cis*-**2** and *trans*-**2** retaining a weak contribution of the O−O bond. *cis*-**2** and *trans*-**2** may be interchanged almost without barrier (TS-**3**, Figure 1B and Figure 6) by a simple in-plane migration of the OH group ($\Delta E^{\ddagger}$+ZPVE = 0.01 kcal/mol) between the two terminal oxygen atoms of the ONO radical fragment (ν = 112.0i cm^{-1}).

The expectation values of the S^2 operator ($\langle S^2 \rangle$ = 0.77 and 0.73) for *cis*-**2** and *trans*-**2** suggest a significant contamination of the singlet wave function with triplet character. A complete active space (CASSCF) calculation was used to assess the multireference character of the wave function. The active space comprised 12 electrons and 10 active orbitals [CAS(12,10)] that included the three σ-bonds of the O−O, O−N, and N−O framework, an in-plane lone pair on oxygen, and the two highest π-orbitals in the occupied space. The virtual orbitals included the three antibonding σ-orbitals and one π-orbital (see Supporting Information). With a 6-311+G(d,p) basis set, the CASSCF optimized geometries of *cis*-**2** and *trans*-**2** were quite close to those obtained with the DFT method (Figure 1B). Another indication of the closeness of the DFT and CASSCF geometries was gleaned from single-point Brueckner Doubles calculations[10a] on the energy differences between the GSs and *cis*-**2** and *trans*-**2**. At the UBD(TQ)/6-311+G(d,p) level, the energy difference between GS *perp*-HO−ONO and *cis*-**2** is 15.1 kcal/mol with the DFT geometry and 14.3 kcal/mol with the CASSCF geometries (Table 1). These energy differences are also in good accord with the DFT energies without ZPVE corrections (Table 1, compare columns A and G). Similarly, the energy difference between minimum GS *perp*-HO−ONO and *trans*-**2** is 13.6 and 12.1 kcal/mol at the DFT and CASSCF geometries. A CIPT2 correlation correction to the CASSCF wave function suggested an energy difference between the GS *perp* and *trans*-**2** of 4.9 kcal/mol. This agrees well with the spin-corrected DFT and G3B3 values given in columns B and E, Table 1. A multireference configuration interaction (MRCI) calculation with the above active space (6.8 million contracted configurations) gave energy differences between GS and metastable conformers of 11.7 and 9.0 kcal/mol for *cis*-**2** and *trans*-**2**. These relative energies garnered by the various methods are summarized in Table 1.

Since the O−O distances in these metastable states are greater than 2 Å and the energy differences between TS_{trans}-**2** and trans minimum **2** are also relatively small, we also examined the potential effect of basis set superposition error (BSSE) using the counterpoise method. We, however, found that comparing total energies of BSSE calculations at the B3LYP/6-311+G(3df,2p) level for both the metastable trans minimum **2** and the corresponding TS_{trans}-**2**, the change in geometry with respect to the non-BSSE structures is negligible. In fact, both optimiza-

Table 2. Calculated Bond Dissociation Energies (BDE = ΔH°_{298}, kcal/mol) at the Different Levels of Theory for Selected Compounds

	B3LYP/6-311+G(d,p)	B3LYP/6-311+G(3df,2p)	G2	G3
HO−**H**	114.8	117.9		118.0
ONO−**H**	74.0	74.3		77.6
O_2NO−**H**	96.8	97.6	106.7	106.3
cis-ONOO−**H**				87.3
cis-ON**O**−**O**H	12.2	16.7		19.1 (19.0)[a]
H_3C−**H**	103.1		105.8	104.1
$(CH_3)_3C$−**H**	92.1	92.0	98.8	96.7
$(CH_3)_2CHCH_2$−**H**	99.0	99.0	103.6	
$(CH_3)_2C{\cdot}CH_2$−**H radical**[b]	38.3			
$(CH_3)_2C$**H**$CH_2{\cdot}$ **radical**[c]	31.4			

[a] The BDE is at the G3B3 level of theory. [b] The BDE is based upon the enthalpy of reaction: isobutene radical → H• + isobutylene. [c] The BDE is based upon the enthalpy of reaction: 2-methylpropyl radical → H• + isobutylene.

tions took only two steps to converge. The final difference in the BSSE corrected energies between these two forms is, $\Delta E = 0.47$ kcal/mol. We have also repeated part of the PES given in Figure 1A (red arrows and numbers) with a somewhat larger (207 versus 165 basis functions) augmented basis set (Aug-cc-pVTZ)[10a] that contains both d and f functions. This exhibits only a minimal basis set effect, and the calculated energy difference between trans GS HO−ONO and TS_{trans}-**2** for O−O bond elongation is 11.0 kcal/mol and between trans GS HO−ONO and *trans*-**2** is 10.8 kcal/mol. The reverse energy barrier for O−O bond elongation (from *trans*-**2** to TS_{trans}-**2**) is slightly reduced to 0.2 kcal/mol with this more flexible basis set (Figure 1).

The O−O bond dissociation enthalpy (BDE) for GS *cis*-HO−ONO is calculated to be 19.1 kcal/mol (ΔH_{298}) at the G3 level of theory (Table 2). The bond energy (BE) based upon G3 total energies is 17.4 kcal/mol. At the G3B3 level the BDE for HO−ONO dissociation is 19.0 kcal/mol and its BE is 17.6 kcal/mol. The B3LYP/6-311+G(3df,2p) calculated dissociation limits for the GS *cis*-, GS *perp*- and GS *trans*-HO−ONO are 17.3, 15.9 and 14.6 kcal/mol. With zero-point energy corrections [ZPE corrections also at B3LYP/6-311+G(3df,2p)] these dissociation limits are 15.3, 14.3, and 13.4 kcal/mol; values were well above the energies of the higher lying minima located. The O−O dissociation limit of 15.3 kcal/mol for GS *cis*-HO−ONO is in good accord with the Gibbs experimental enthalpy and free energy of activation (18 ± 1 kcal/mol, $\Delta S^\ddagger = 3$ eu and 17 ± 1 kcal/mol, $\Delta S^\ddagger = 12$ eu) for the isomerization of peroxynitrite to its nitrate form (presumably by a dissociative mechanism). However, the calculated Gibbs free energies for dissociation of *cis*-HO−ONO (5.9 kcal/mol, $\Delta S = 36$ eu) are significantly less than the experimental value for O−O dissociation in solution. While gas-phase and solution entropies are not directly comparable, the existence of *cis*-**2** and *trans*-**2** in the gas phase remains an open question. These same arguments have been used to question the relevance of weakly bound complexes of NO_2 and hydroxyl radical suggested earlier by Houk[7c] to represent the so-called "excited" structure of HO−ONO*. The stability of these isomeric hydrogen-bonded radical pairs (**4A** and **4B**, Figure 1B) was recently questioned by Musaev.[15a] On the basis of B3LYP, MP2, and CCSD calculations it was suggested that such hydrogen bonded structures (•OH····ONO•) of dissociated peroxynitrous acid (including zero-point energy and entropy corrections) do not exist in the gas phase.

The relative energies of the metastable forms of HO−ONO, *cis*-**2**, and *trans*-**2** versus the isomeric H-bonded complexes **4A** and **4B** remain an important mechanistic issue especially if either class of compound is involved in hydrocarbon oxidation. In principle, the "excited" singlet isomers of HO−ONO could rearrange with a very small activation barrier to hydrogen bonded isomers **4A** and **4B**. However, this PES is very flat, and we were unable to locate the transition structures for rearrangement of these very loosely bound structures. Our initial series of calculations with the B3LYP calculations and more highly correlated methods (Table 1) all suggest that H-bonded complexes **4A** and **4B** are several kcal/mol *higher* in energy than *cis*-**2** with and without solvent correction (COSMO).

The G3 and G3B3 protocols have been shown to provide experimental accuracy for the bond energies in a number of relatively small molecules albeit with normal covalent bonding interactions. Since the standard G3B3 method employs a series of higher level single-point energy corrections on geometries optimized at B3LYP with the relatively small 6-31G(d) basis set, we opted to improve upon this standard procedure by using a higher quality basis set [6-311+G(3df,2p)] for the initial geometry optimization and frequency as described above in the Computational Details section. The G3//B3LYP/6-311+G(3df,-2p) O−O BE for GS *cis*-HO−ONO is 17.6 kcal/mol (almost identical to the G3B3 value). The O−O BDE for this GS peroxynitrous acid at the G3 and B3G3 are very close (19.1 and 19.0 kcal/mol, Table 2). This suggests that neither the method of geometry optimization nor the quality of the basis set has a significant effect. However, with the G3B3//B3LYP/6-311+G(3df,2p) method, we find that H-bonded complexes **4A** and **4B** are slightly more stable (1.4 kcal/mol) than *cis*-**2** and 6.4 kcal/mol less stable if spin corrections are applied within the G3B3 computational scheme (Table 1, columns D and E). We conclude, based upon this level of theory, that both isomeric forms of HO−ONO are of comparable energy in the gas phase.

Our ability to locate these higher lying singlets of peroxynitrous acid is largely a consequence of the fact that we were able to discourage the wave function from converging on closed-shell solutions (zero spin densities) during geometry optimization by using guess = mix[10a] which forces, initially, HOMO and LUMO to be mixed so as to destroy $\alpha-\beta$ and spatial symmetries. Having demonstrated the potential effects of BSSE and the influence of a more flexible basis set, it would now seem prudent to examine the possible influence of spin contamination. We have up to now assumed that the resulting open-shell description is at least qualitatively satisfactory in terms of calculated spin densities and that the structures in Figure

(15) (a) Musaev, D. G.; Hirao, K. *J. Phys. Chem. A.* **2003**, *107*, 1563. (b) Musaev, D. G.; Geletii, Y. V.; Hill, C. L. *J. Phys. Chem. A.* **2003**, *107*, 5862.

1 are reasonable. It is evident from the $\langle S^2 \rangle$ values in Table 1 that the extent of triplet contamination in the UDFT monodeterminantal wave function is significant. In some cases such as H-bonded complexes **4A** and **4B**, where the $\langle S^2 \rangle$ values are approaching unity, the wave function is essentially an equal mixture of singlet and triplet spin multiplicities and the total energies are no longer reflective of the assigned singlet state and need to be corrected. The spin-projection method of Yamaguchi,[12b,c] although controversial for DFT calculations,[12d] was designed to refine the total energy by elimination of the spin contamination from the singlet wave function for MPn calculations. A comparison of the *relative* energies of the uncorrected minima and TSs in column A (Table 1) with those with the spin-contamination corrected UB3LYP/6-311+G(3df,-2p) energies in column B shows a considerable reduction in the energy differences between GS *cis*-HO−ONO and *cis*- and *trans*-**2** (5.8 and 5.4 kcal/mol). The latter value is now in close agreement with the CIPT2 corrected CAS(12,10)/6-31+G(d,p) energy for *trans*-**2** (4.9 kcal/mol, column F). Significantly, this energy correction places the H-bonded minima **4A** and **4B** much higher in energy relative to *cis*- and *trans*-**2**. When the *relative* energies for the presumably more accurate G3B3//B3LYP/6-311+G(3df,2p) [column D] are corrected for spin-contamination [column E], the results mirror those without the G3B3 energy correction scheme in column B and suggest that *cis*- and *trans*-**2** are 6−9 kcal/mol more stable than **4A** and **4B**. A list of the series of MPn calculations involved in the G3B3 protocol is given in the Computational Details section. Since the Yamaguchi correction[12b] depends on the calculated energy difference between the singlet and triplet states (see Computational Details section), this energy difference (S−T, kcal/mol), as well as the $\langle S^2 \rangle$ value, is important. It is worthy of note that the singlet−triplet energy differences for the TSs involved in Figure 1 are greater than those of the minima with the exception of H-bonded minima **4A** and **4B** where $\langle S^2 \rangle = 1$ but the singlet−triplet energy difference is essentially zero and hence the Yamaguchi correction is very small. This is not that surprising since **4A** and **4B** are essentially separated radicals with oxygen−oxygen distances of 3.194 and 3.168 Å. Finally we point out that the corrections to the Brueckner Doubles calculations [BD(TQ)] also afford relative energies [column G] that support the basic contention that *cis*- and *trans*-**2** exist as discrete minima on this PES (Figure 1).

From a biochemical perspective the more important question is the relative stability in aqueous solution. The relationship of the above gas-phase calculations to HO−ONO under physiological conditions now becomes the more relevant question. While we cannot address this question directly, we have carried out full geometry optimizations of *cis*- and *trans*-**2** using the COSMO solvent model.[10a,12] In THF solvent the energy difference between GS *cis*-HO−ONO and *cis*-**2** and *trans*-**2** was 12.3 and 10.2 kcal/mol [B3LYP/6-311+G(d,p)]. The energy differences between the GSs and their metastable forms with this smaller basis set in the gas phase are 12.2 and 9.9 kcal/mol. In methanol solvent these energy differences increased to 13.9 and 12.4 kcal/mol, and in water media the energy increases were 14.3 and 12.7 kcal/mol [15.4 and 14.2 kcal/mol with the larger 6-311+G(3df,2p) basis set]. Significantly, *cis*-**2** and *trans*-**2** both exist as energy minima in polar media with elongated O−O distances (2.140 and 2.089 Å) for *cis*-**2** and *trans*-**2** in water (COSMO solvent model).

Since hydrogen bonding is not explicitly treated in the COSMO solvent model, we examined the stability of *trans*-**2** H-bonded to several water molecules. We located minima for *trans*-**2** H-bonded to one, two, three, and four H_2O molecules (see Supporting Information) with O−O distances of 2.13, 2.12, 2.15, and 2.11 Å [B3LYP/6-311+G(d,p)]. As anticipated the overall complexation energy increased almost linearly with increasing numbers of H_2O molecules (−5.6, −15.9, −28.2, and −34.7 kcal/mol). The water molecules exhibited very little affinity for O−N−O with all of the H-bonding being to the hydroxyl fragment. A water molecule placed near the O−N−O fragment migrates to the vicinity of the nearest hydroxyl group. Optimization of *cis*-**2** H-bonded to three waters resulted in a *perp*-**2**·$3H_2O$ complex (Figure 2, ∠HOON = 68°). The energy difference between this complex and *trans*-**2** H-bonded to $3H_2O$ is only 0.3 kcal/mol (Figure 2).

By contrast the weak interaction between the hydrogen bonded (•OH···ONO•) radical pairs in **4A** and **4B**[6c] (Figure 1B) completely dissociates upon inclusion of just two H_2O molecules.[15a] At the G3B3//B3LYP/6-311+G(3df,2p) level the hydroxyl radical in **4A** and **4B** is bound to the ONO radical in the gas phase by only 1.12 and 1.07 kcal/mol. Both *cis*- and *trans*-GSs of HO−ONO when H-bonded to $3H_2O$ result in perpendicular complexes (Figure 2, ∠HOON = 91.4° and 116.2°, ΔE = 0.3 kcal/mol). The energy difference between *trans*-**2**·$3H_2O$ and the corresponding GS *perp*-HO−ONO·$3H_2O$ is 12.1 and 12.2 kcal/mol for the *perp*-**2**·$3H_2O$ complex thereby supporting the existence of these higher lying singlets in aqueous media (Figure 2). When GS *perp*-HO−ONO·$3H_2O$ and its metastable form H-bonded to three waters are optimized within the COSMO solvent model (solvent = water), the metastable *trans*-**2**·$3H_2O$ form is 12.9 kcal/mol (12.8 kcal/mol with ZPE) higher in energy than GS *perp*-HO−ONO·$3H_2O$ compared with 12.1 kcal/mol in the gas phase. We suggest that solvated forms of *cis*-**2**·$3H_2O$ and *trans*-**2**·$3H_2O$ represent the elusive higher lying biradicaloid minima that have been advocated as the metastable forms of peroxynitrous acid (HOONO*)[2,3] largely responsible for the rich chemistry associated with this highly reactive oxidant. We base this conclusion largely on the basis of the presumed stability of *cis*-**2** and *trans*-**2** in aqueous solution.

(b) Origin of the Stability of the Metastable States of HO−ONO. The O−O bond in the higher lying singlet HO−ONO is unquestionably a unique σ-bond, and the origin of this type of metastable peroxide requires an explanation. First, it should be recalled that this type of "excited" O−O σ-bond is not entirely unexpected, since it is well established that the simplest cyclic peroxide, dioxirane, has several higher lying singlet minima where the O−O bond is elongated above that in its ground state. In the case of dioxiranes the electrons of the O−O σ-bond and the oxygen lone pairs in the GS and in the respective dioxymethane biradicals (O−CH_2−O) occupy different spatial orientations, represent different electronic states, and consequently meet the definition of an excited state. Using the Goddard nomenclature,[16a] ground-state dioxirane and its low-

(16) (a) Wadt, W. R.; Goddard. W. A., III. *J. Am. Chem. Soc.* **1975**, *97*, 3004. (b) Bach, R. D.; Andres, J. L.; Owensby, A. L.; Schlegel, H. B; McDouall, J. J. W. *J. Am. Chem. Soc.* **1992**, *114*, 7202. (c) Anglada, J. M.; Bofll, J. M.; Olivella, S.; Sole, A. *J. Chem. Phys.* **1998**, *102*, 3398.

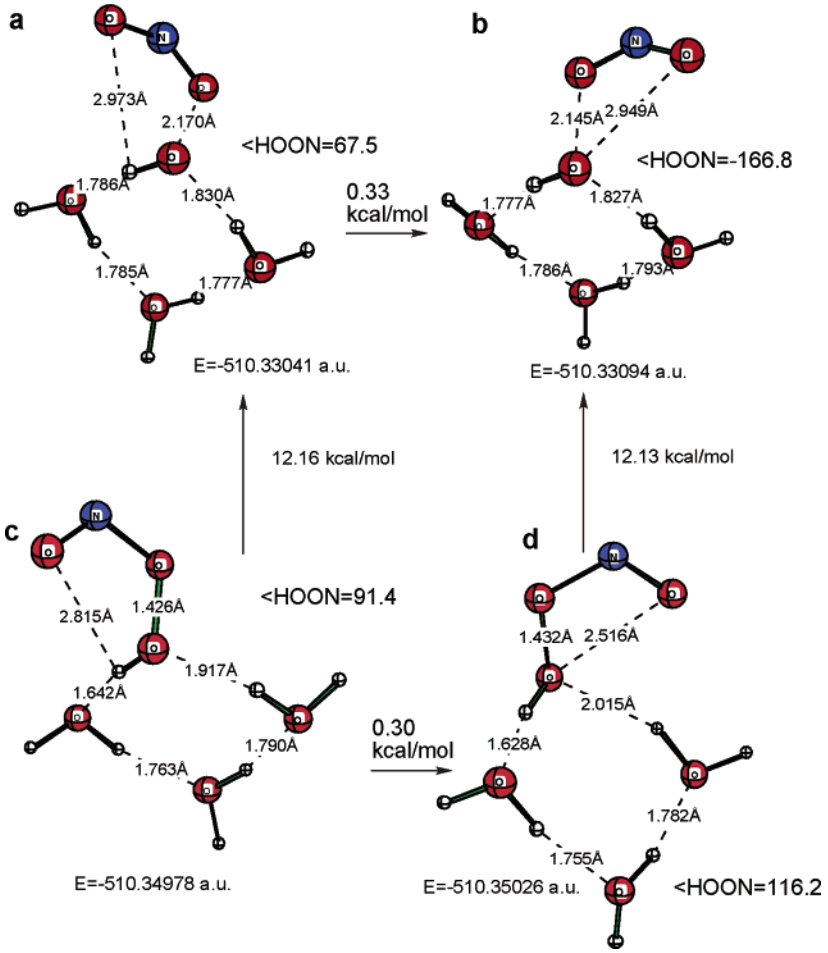

Figure 2. UB3LYP/6-311+G(d,p)-optimized structures of *cis*- and *trans*-**2** H-bonded to $3H_2O$ (a, b) and their corresponding RB3LYP/6-311+G(d,p)-optimized *cis*- and *trans*- ground-state HO−ONO isomers (c, d).

lying 2π, 3π, and 4π excited states are all discrete singlet minima with different O−O bond distances (1.530, 2.350, 2.138, and 2.203 Å)[16b] and relative energies.[16c] It was, in fact, just this set of excited minima and how one can arrive at these excited states[16b] that guided us in the present study. Second, it is instructive to compare the electronic properties of the NO_2 radical with those obtained upon homolytic O−O bond dissociation in other peroxides. In an earlier report[8b] we assigned an O−O BDE (ΔH_{298}) for HO−ONO of 22 kcal/mol (G2) as compared to the much stronger O−O bonds in CH_3O−OH (ΔH_{298} = 45 kcal/mol) and peroxyformic acid, H(C=O)O−OH (ΔH_{298} = 48 kcal/mol). First we will provide a rationale for these rather remarkable differences in BDE using the DFT method. Rauk has shown that MPn calculations gave the same order of states as CASPT2 calculations,[7a] and it has been established that B3LYP calculations are capable of adequately treating the symmetry breaking and zero-point energy problems associated with this type of radical. This DFT variant has been used successfully to analyze such problems[8b,7a] and will consequently be used in the present study.

In addition to the OH radical, homolytic O−O bond dissociation of methyl hydroperoxide (CH_3O−OH) produces the CH_3O oxyradical that has two competitive electronic states (2A′ and 2A″) that are nearly degenerate.[8b] Thus, the spatial orientation of the electron spin on the oxyradical cannot influence the stabilization of the RO oxyradical, and hence, CH_3O−OH has a normal O−O bond energy (45 kcal/mol).

Scheme 1

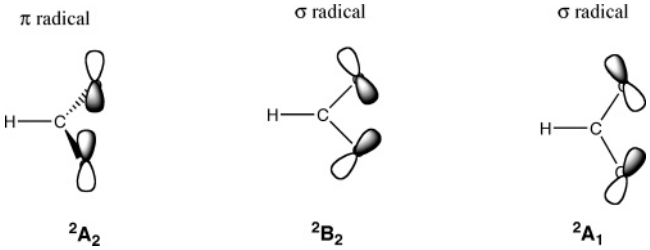

However, both alkyloxyl (RCO_2) and NO_2 radicals have a σ ground state, and both σ and π types of radicals suffer from problems of symmetry breaking. The $^2B_2$ state of HCO_2 radical has two closely related σ orbitals. The $^2B_2$ state is the minimum, lying just 2.3 kcal/mol below the $^2A_1$ σ state (Scheme 1).[7a]

The π states are significantly higher in energy than the σ states. The calculated energy difference between the lower lying σ and π states ($\sigma\,^2B_2 - \pi^2A_2$) was 10.9 kcal/mol for the HCO_2 radical and 14.5 for CH_3CO_2. Significantly, upon homolytic O−O bond dissociation RCO_2−OH provides alkyloxy radicals that correlate with their σ ground states. For peracids the higher lying $^2A_2$ π state, where the electron spin is delocalized up in the π system, does not provide an opportunity for any special type of stabilization, and hence peracids have rather typical O−O BDE (47−48 kcal/mol).[8b]

Another type of peroxide bond where a unique opportunity exists for resonance stabilization of an oxy radical is where the

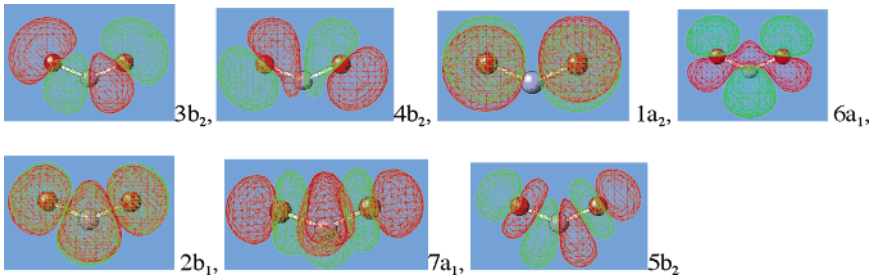

Figure 3. Characteristic occupied and virtual orbitals for the $^2A_1$ state of NO_2 optimized at the UB3LYP/6-311+G(d,p) level of theory. Alpha orbitals: (occupied) ...$3b_2$ $4b_2$ $1a_2$ $6a_1$; (virtual) $2b_1$ $7a_1$ $5b_2$. Beta orbitals: (occupied) ...$3b_2$ $1a_2$ $4b_2$; (virtual) $6a_1$ $2b_1$ $7a_1$ $5b_2$.

oxygen radical is conjugated to a carbon−carbon double bond. We reported earlier that simple vinyl hydroperoxides (H_2C═CHO−OH) such as isopropenyl hydroperoxide had an atypically low O−O BDE due to the delocalization of the O-centered radical to a C-centered radical.[8b] Cleavage of the O−O bond in isopropenyl hydroperoxide produces a putative isopropenyloxy radical with the spin on oxygen oriented in the σ plane of the molecule ($\sigma\ ^2A'$) that corresponds to an O−O BDE of 42.9 kcal/mol (G3). However, in this case and in direct contrast to the aforementioned O−O dissociation of peroxyformic acid (Scheme 1), the electronic spin density prefers to reside on the carbon atom resulting in a stabilization energy of 23.1 kcal/mol ($\Delta E_{\delta\pi}$, G3) due to electron delocalization in the π system. Equilibrium O−O bond dissociation correlates with the lower lying $\pi\ ^2A''$ state, and the O−O BDE is dramatically reduced to 19.6 kcal/mol (G3). The lesson to be gleaned from this discourse is that O−O bond dissociation attended by some form of unique stabilization of the alkoxy radical produced can be directly responsible for an exceptional type of atypically weak peroxy bond. Just such an extraordinary reduction in bond dissociation energy accompanies homolytic O−O bond cleavage in HO−ONO!

In the case of HO−ONO we do not have a competition between σ and π states of different energies, but rather between two σ states. The NO_2 radical correlates with a low lying σ type orbital that undergoes both electronic and geometric reorganization upon O−O bond cleavage resulting in a very low O−O bond dissociation energy. The NO_2 radical has been thoroughly studied starting with the seminal paper by Davidson.[17] The ground state of NO_2 is $^2A_1$ that has an O−N−O bond angle of 134°.

The $^2A_1$ orbital of NO_2 is nominally an in-plane nitrogen-centered orbital with a symmetric but smaller in-plane contribution of the oxygen lone pair orbitals (6a1, Figure 3) where the spin density is localized extensively on the nitrogen atom (Figure 4 and Table 3). The electron distribution in this MO is approximately evenly distributed between the two oxygen atoms and the nitrogen atom.

The higher lying first excited $^2B_2$ state of NO_2 is characterized by orbital $4b_2$ which is an antibonding combination of the in-plane oxygen lone pair orbitals, the $6a_1$ orbital is doubly occupied thereby providing a much smaller O−N−O angle of 102° due to its bonding character (Figure 4).

The $^2B_2$ orbital of the NO_2 radical has a different spin density with a larger contribution from the two oxygens. This higher energy state with an O-centered orbital is calculated to be 41.4,

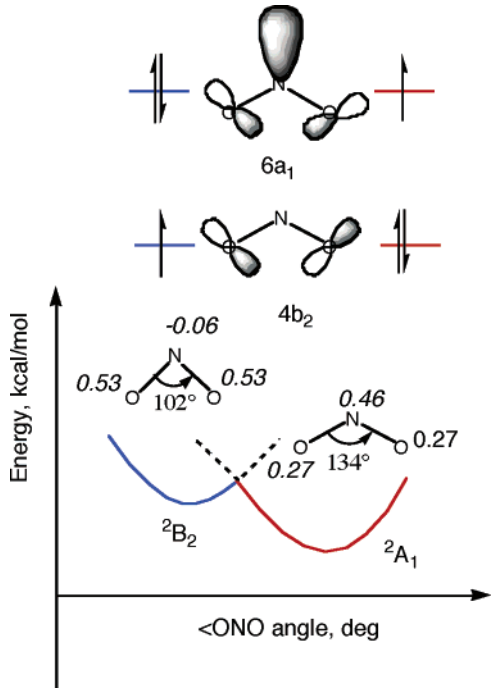

Figure 4. Schematic presentation of the $^2B_2$ and $^2A_1$ states of the NO_2 radical. Total atomic spin densities for the $^2B_2$ and $^2A_1$ states of the NO_2 radical are shown as italic numbers [UB3LYP/6-311+G(3df,2p)].

Table 3. Total Atomic Spin Densities for the $^2B_2$ and $^2A_1$ States of NO_2 Radical at the UB3LYP/6-311+G(3df,2p) Level

atom	$^2A_1$	$^2B_2$
N	0.455	−0.065
O	0.272	0.532
O	0.272	0.532

28.4, 29.0, and 30.2 kcal/mol less stable than GS$^2A_1$ at the B3LYP/6-311+G(3df,2p), CBS-Q, G3B3, and MRCI+Q/cc-pVQZ[18a] levels of theory.

A fundamental question is why the higher lying metastable singlet of HO−ONO, *cis*-**2**, does not simply collapse to ground state *cis*-HO−ONO? Both metastable *cis*- and *trans*-**2** "excited" state peroxides have the same symmetry (A') but a different electron spin distribution relative to ground-state HO−ONO. At some point during the O−O bond elongation process the electron of the developing ONO radical fragment shifts from being localized largely on the oxygen of the O−O bond to the central nitrogen atom of the ONO fragment thereby relaxing to

(17) (a) Davidson, E. R. *J. Am. Chem. Soc.* **1977**, *99*, 397. (b) for recent studies on potential energy surfaces of NO_2, see refs 18.

(18) (a) Kurkal, V.; Fleurat-Lessard, P.; Schinke, R. *J. Chem. Phys.* **2003**, *119*, 1489. (b) Mahapatra, S.; Köppel, H.; Cederbaum, L. S.; Stampfuss, P.; Wenzel, W. *Chem. Phys.* **2000**, *259*, 211. (c) Hirsch, G.; Buenker, R. J.; Petrongolo, C. *Mol. Phys.* **1991**, *73*, 1085. (c) Salzgeber, R. F.; Mandelshtam, V.; Schlier, C.; Taylor, H. S. *J. Chem. Phys.* **1998**, *109*, 937.

Table 4. Total Atomic Spin Densities for Metastable HO−ONO* *cis*-**2** and *trans*-**2** Structures Optimized at the UB3LYP/6-311+G(3df,2p) Level

atom	*cis*-**2**	*trans*-**2**
O	−0.196	−0.224
N	−0.464	−0.452
O	−0.183	−0.140
O	0.870	0.842
H	−0.026	−0.0261

the ground $^2A_1$ state and recovering a part of the potential energy associated with this $^2B_2$ to $^2A_1$ electronic reorganization. In both *cis*- and *trans*-**2** the electron spin of the OH fragment is still in the plane (A′ symmetry). As the O−O bond elongates, the O−N−O angle widens as it approaches the 134° of the $^2A_1$ minimum with a consummate lowering of the total energy of *cis*-**2**. It is this electronic reorganization attending O−O bond elongation that is responsible for the stabilization of the metastable state of peroxynitrous acid (HO····ONO*) and hence its short-lived existence.

Although ground state *cis*-HO−ONO has an O−N−O angle of 115° [UB3LYP/6-311+G(3df,2p), CAS(12,10)/6-311+G(d,p)], examination of Figure 4 shows that this angle places the O−N−O fragment between the $^2B_2$ and $^2A_1$ surfaces. Examination of the HOMOs of *cis*-**2** and *trans*-**2** shows that there is a large contribution from the nitrogen orbital, as noted for the NO_2 radical itself. This is also evident from the total atomic spin densities for *cis*-**2** and *trans*-**2** (Table 4, Figure 5).

The LUMO orbitals are antibonding combinations of the 6a1 orbitals of ONO and in-plane lp(O) of OH. Electron occupations of LUMO for *cis*-**2** and *trans*-**2** are 0.61 and 0.68. A full electron is not transferred to LUMO during O−O bond elongation. Thus, peroxynitrous acid represents an exceptional type of peroxide where O−O bond cleavage is attended by a unique stabilization of one of the resultant radical fragments.

(c) The Rearrangement of Peroxynitrous Acid to Nitric Acid. One of the primary reactions of peroxynitrous acid observed in aqueous solution is its rapid exothermic (ΔE = −29.1 kcal/mol, G3; ΔE = −29.4 kcal/mol, G3B3) rearrangement to nitric acid. The reaction enthalpies for this rearrangement by these two closely related methods are −29.2 and −29.6 kcal/mol. The energy of the so-called "excited" form of peroxynitrous acid (HO−ONO*) has been estimated to be approximately the same as the experimental activation barrier for the HO−ONO → HO−NO_2 rearrangement barrier (∼ 17 kcal/mol).[2,3] Since this rearrangement exhibits a very high calculated barrier for a *concerted* 1,2-OH shift, it could potentially involve O−O bond dissociation with a simple recombination. Consequently, we elected to briefly revisit the rearrangement of HO−ONO to nitric acid (path b, Scheme 2) to examine the potential role of metastable peroxynitrous acid (*cis*-**2**) that might exhibit a lower barrier on the open-shell surface.

Location of the TS for this formal 1,2-OH shift has proven to be difficult but both Peyerimhoff et al.[6a] and Dixon et al.[6b] have reported activation barriers of 39.0 kcal/mol (B3LYP) and 21.4 kcal/mol (MP2/cc-pVTZ). Presumably the latter second-order perturbation method does not treat the diradical nature of the TS adequately.[6b] This MP2 TS was rather loose and had an OH to central nitrogen of the ONO fragment distance of 2.78 Å. These relatively high level calculations also suggest that the energy to form OH + NO_2 from HO−ONO dissociation is 19.8 kcal/mol if all calculated values are used and 18.3 kcal/mol if mostly experimental values are used.[6b]

We initiated the potential rearrangement from GS *cis*-HO−ONO and observed an activation barrier of 41.2 kcal/mol [B3LYP/6-311+G(3df,2p)+ZPVE]. The O−O distance was 2.53 Å with an O−N distance of 2.38 Å in the transition state for OH to migrate from O to N in the NO_2 fragment of HO−NO_2 (Figure 6). In the TS the OH is essentially stationary between the two ONO oxygen atoms, and animation of the single imaginary frequency (ν_i = 704.1i cm^{-1}) showed largely a rocking motion of the ONO nitrogen toward the OH group. This concerted rearrangement takes place on the restricted PES as a pure singlet ($\langle S^2 \rangle = 0.0$) despite our repeated attempts to the contrary initiating the TS search with a wave function having $\langle S^2 \rangle = 1.0$ (guess = mix). While the magnitude of the barrier may seem surprisingly high for such a loosely bound TS, it should be remembered[8c] that all such concerted 1,2-rearrangements to a lone pair of electrons are four-electron processes that are formally forbidden and hence typically exhibit very high barriers well in excess of 40 kcal/mol. For example, the barrier for the 1,2-hydrogen shift in hydrogen peroxide to form water oxide is 55 kcal/mol.[8d] Thus, all three theoretical studies[6a,b] suggest that the facile rearrangement of HO−ONO to HO−NO_2 involves O−O bond dissociation to its free radical components followed by some form of recombination. The calculated concerted rearrangement barrier is simply too high to be consistent with experiment. Presumably the first step in this dissociative pathway involves the TS for O−O cleavage (TS_{cis}-**1**) to *cis*-**2** followed by solvation to a radical pair that can recombine to isomeric nitric acid essentially without a barrier. Since completion of this work Houk and co-workers[19] have suggested that H-bonded complex **4B**, formed prior to recombination to nitric acid, might be among the species exhibiting the HO−ONO* behavior of one-electron oxidation processes. The potential involvement of hydrogen bonded complexes **4A** and **4B** (Figure 1) in biological reactions remains an open question in aqueous media.

(d) Oxidation of Methane with Metastable Peroxynitrous Acid. Two fundamental questions of pertinence to the chemistry of higher lying metastable states of peroxynitrous acid are their relative stability in aqueous media and possible involvement in biological reactions. We have attempted to answer the former question by showing that HO−ONO* would be stable in a polar environment using the COSMO solvent model and by an explicit examination of these metastable states in the presence of several water molecules. We have previously shown that GS HO−ONO can be involved in such two-electron processes as alkene epoxidation and the oxidation of amines, sulfides, and phosphines.[8a] There has also been a controversy about the mechanism of HO−ONO oxidation of saturated hydrocarbons. Rauk et al.[7a] have advanced the hypothesis that the reactive species in hydrocarbon oxidations by peroxynitrous acid, and in lipid peroxidation in the presence of air, is the discrete hydroxyl radical formed in the homolysis of HO−ONO. The RB3LYP/6-31+G* wave functions for a series of TSs involving C−H oxidation with HO−ONO were found to suffer from an RHF→UHF instability. However, attempted reoptimizations on the unrestricted PES (UB3LYP) produced structures identical

(19) Zhao, Y.; Houk, K. N.; Olson, L. P. *J. Phys. Chem. A* **2004**, *108*, 5864.

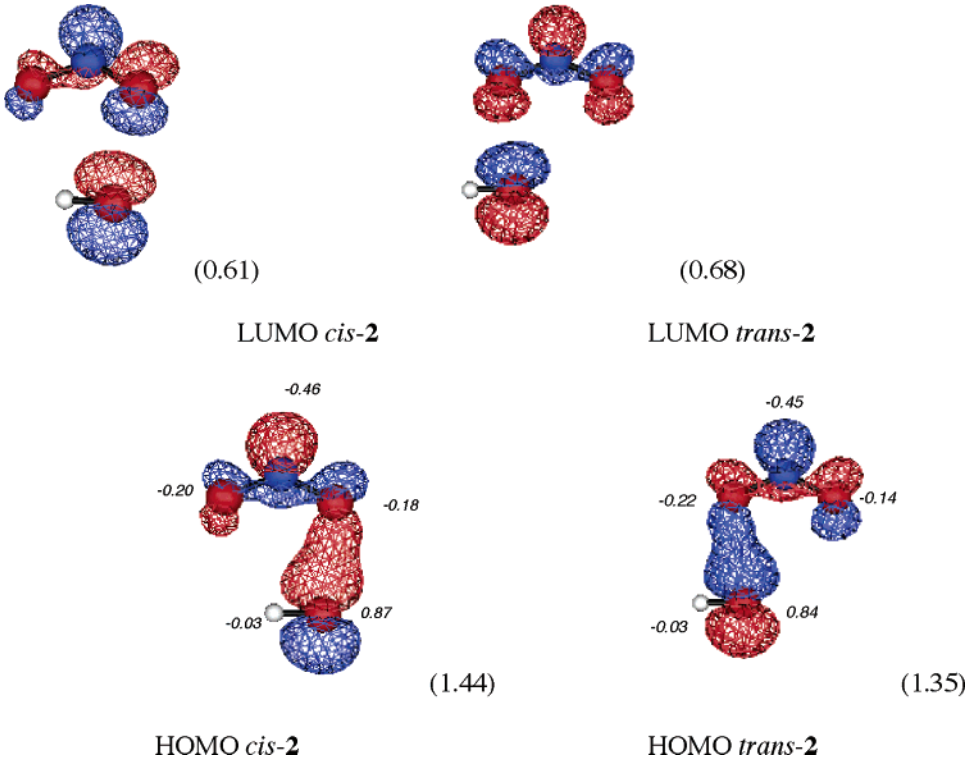

Figure 5. Highest occupied and lowest unoccupied orbitals (HOMO and LUMO) of *cis*-**2** and *trans*-**2** optimized at the CAS(12,10)/6-311+G(d,p) level. Electron occupations are given in parentheses. Italic numbers correspond to total atomic spin densities in the structures optimized at the UB3LYP/6-311+G-(3df,2p) level.

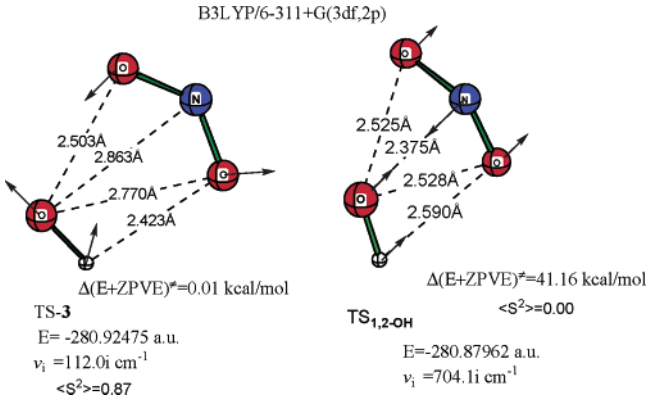

Figure 6. Transition structures (UB3LYP/6-311+G(3df,2p)) for the isomerization of metastable *cis*-**2** to *trans*-**2** (TS-**3**) and the isomerization of ground-state HO−ONO to nitric acid, HO−NO$_2$(TS$_{1,2-\mathbf{OH}}$), optimized at the RB3LYP/6-311+G(3df,2p) level of theory.

Scheme 2

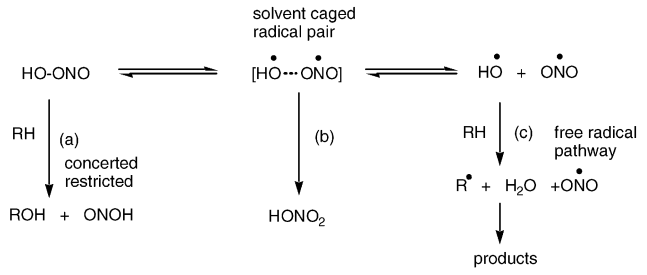

in geometry and energy to those at RB3LYP.[7a] Geletii and co-workers[7d] have also presented arguments that alkane oxidation can proceed in both the gas phase and the liquid phase. These data were extended to include similar processes in lipophilic media.

We initiated our study with the HO−ONO oxidation of methane (eq 1)

$$\mathrm{HOONO} + \mathrm{CH_4} \rightarrow \mathrm{CH_3OH} + \mathrm{HONO} \qquad (1)$$

by first reexamining the RB3LYP surface (Scheme 2) and then making a comparison with the PES on the UB3LYP surface.[9]

Our RB3LYP surface for concerted methane oxidation was essentially identical to that previously reported[7a] with the differences being due a slightly different basis set. At the RB3LYP/6-311+G(d,p) level we calculate a classical activation barrier for methane oxidation of $\Delta E^{\ddagger} = 31.1$ kcal/mol (TS-$\mathbf{6_R}$ Figure 7). The HO−ONO oxidation of methane on the restricted surface with the B3LYP and QCISD methods gave similar values of activation energy (31 ± 3 kcal/mol) irrespective of basis set size;[7a] attempted reoptimization of these TSs on the UB3LYP PES gave an identical solution with $\langle S^2 \rangle = 0.0$.

We have chosen not to address directly the free radical pathway (Scheme 2, path c) since this has been thoroughly studied by Rauk.[7a] The next issue to resolve is whether hydrogen abstraction with this metastable HO−ONO*/methane complex on the unrestricted surface (Scheme 3) is possible, and to determine if this pathway is a higher or lower energy process than the concerted two-electron closed-shell oxidation from GS HO−ONO.

For comparison of the relative energetics of this overall oxidation we chose GS HO−ONO (*cis*-conformer with this method) and methane as the isolated reactants. The initial prereaction complex (MIN-**5**) between GS HO−ONO and CH$_4$ is stabilized by 0.4 kcal/mol (Figure 7). This is a rather loose complex stabilized by three weak H-bonds (two CH····OH and one CH····ONO, Figure 7) and a distance between the peroxynitrous acid OH group and the C of methane of 3.55 Å. As in

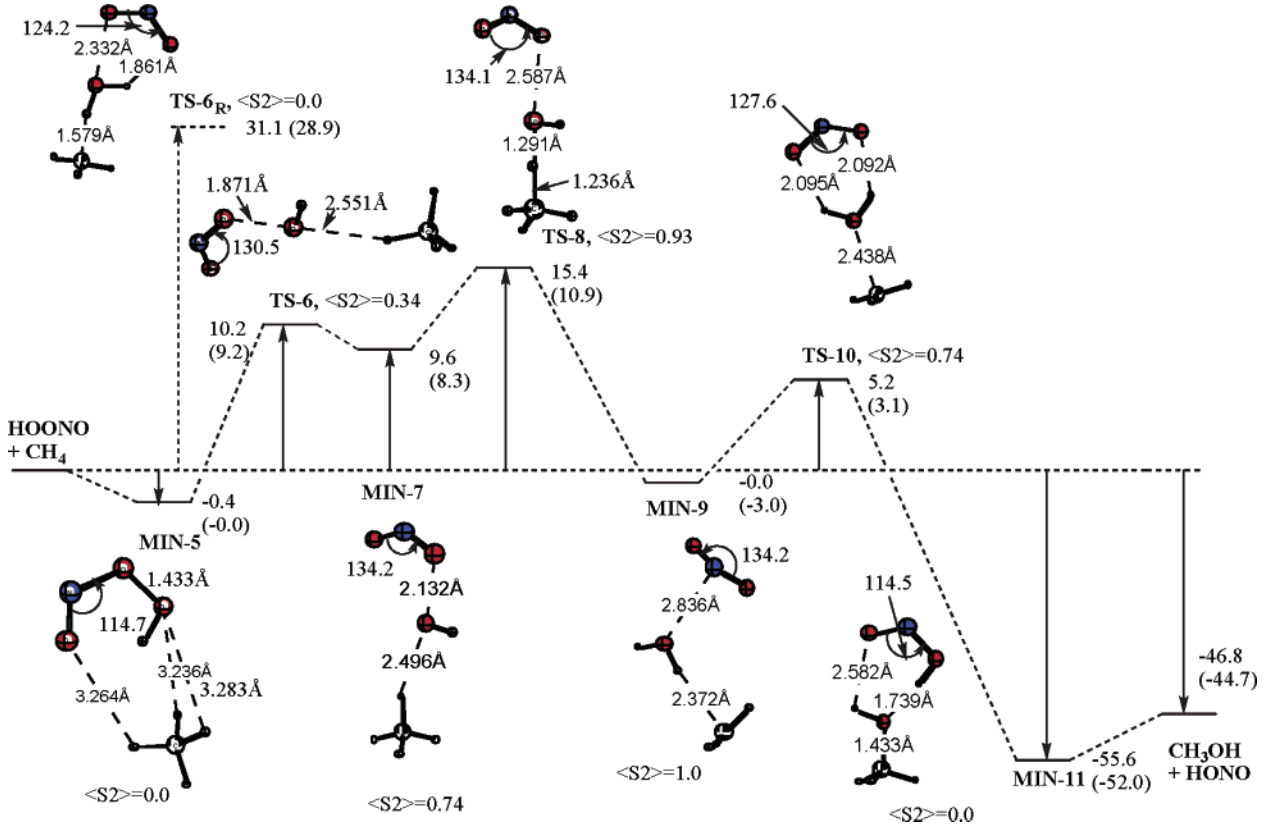

Figure 7. B3LYP/6-311+G(d,p) energy diagram for the HO−ONO oxidation of CH_4 to produce methanol. Relative energies in kcal/mol are with respect to isolated reactants (values in parentheses are with ZPE correction): prereaction complex of GS HO−ONO and methane, MIN-**5** (−321.460 89 au); transition structure for hydrogen abstraction from methane on the closed-shell surface, TS-$\mathbf{6_R}$ (−321.410 79 au); TS for O−O bond elongation on the unrestricted surface, TS-**6** (−321.443 98 au); MIN-**7** (−321.444 98 au); transition structure for hydrogen abstraction from methane, TS-**8** (−321.435 79 au); MIN-**9** (−321.460 31 au); transition structure for the hydroxylation of methyl radical, TS-**10** (−321.452 09 au); product complex of methanol and HONO, MIN-**11** (−321.548 95 au).

Scheme 3

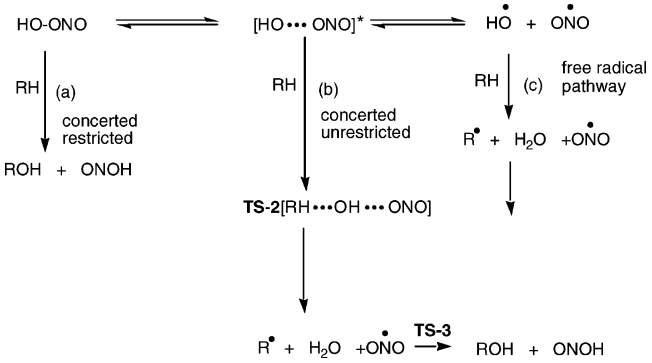

the HO−ONO molecule itself, we were also able to locate a transition state (TS-**6**) for the O−O bond elongation process, *where the developing HO−ONO* is complexed to a methane molecule* (C····O distance 3.54 Å). Metastable O-O bond elongation TS-**6** is 10.2 kcal mol^{-1} higher than isolated reactants and has $\langle S^2\rangle = 0.34$. The structure of the HOONO fragment is almost identical with the TS for formation of *trans*-**2** itself from GS HO−ONO (TS_{trans}-**2**) with an O−O bond distance of 1.889 Å and a $\langle S^2\rangle = 0.44$. A subsequent IRC calculation confirmed that this TS connects the initial prereaction complex (MIN-**5**) with the product complex (MIN-**7**) with a structure similar to the trans-**2** minimum and a CH_4 molecule interacting with the OH group (C····O distance 3.53 Å). Significantly, this "excited state" prereaction complex is only 9.6 kcal/mol above isolated reactants (Figure 7). The difference in energy between MIN-**7** and TS-**6** is only 0.6 kcal mol^{-1} and an $\langle S^2\rangle = 0.74$ is consistent with its biradicaloid nature. The HO−ONO* fragment in MIN-**7** has an O−O distance of 2.13 Å and an overall structure nearly identical to that of *trans*-**2**. It is also significant that a weak O−O bonding interaction is still in evidence, a feature that is conspicuously absent in H-bonded complexes **4A** and **4B**. Presumably we arrive on the PES of the trans metastable isomer, since *trans*-**2** itself is 1.6 kcal/mol lower in energy than *cis*-**2** (Figure 1).

It was gratifying to locate a TS for H abstraction from methane on the unrestricted PES because this provides corroborative evidence for the earlier suggestion[2,3] that metastable forms of HO−ONO can play a role in biochemical processes. The highest point on the PES for methane oxidation is the transition state for hydrogen abstraction by the *weakly bound* hydroxyl radical (TS-**8**). This key TS for the oxidation step is located 5.8 kcal mol^{-1} higher than trans MIN-**7** but is 15.8 kcal/mol higher in energy than prereaction minimum MIN-**5**. This is clearly a biradicaloid transition structure, since it has $\langle S^2\rangle = 0.93$ with a geometry that closely resembles the TS for methane H abstraction by OH radical itself (TS-**12**, Figure 8). Hydrogen abstraction from methane by isolated hydroxyl radical has an activation barrier of only 2.3 kcal/mol compared to the HO−ONO* barrier of 15.4 kcal/mol (TS-**8**). By contrast, the NO_2 radical exhibits a very low propensity for hydrogen abstraction from methane exhibiting a corresponding activation barrier of 33.2 kcal/mol (TS-**13**, Figure 8).

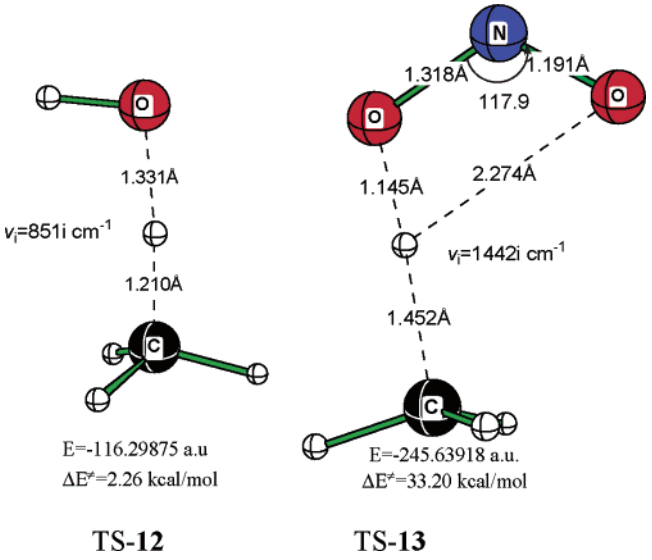

Figure 8. Transition structures for hydrogen abstraction from CH_4 by OH radical (TS-**12**) and ONO radical (TS-**13**) optimized at the UB3LYP/6-311+G(3df,2p) level of theory. The classical energy barriers ($\Delta E^{\ddagger}$) are based upon total energies of the isolated reactants and the corresponding TSs. $E(OH^{\bullet}) = -75.765\,57$ au; $E(CH_4) = -40.536\,79$ au; $E(ONO^{\bullet}, {}^2A_1) = -205.155\,30$ au.

Following the IRC from TS-**8** toward products, we located MIN-**9**, a structure than can be formally described as NO_2 and CH_3 radicals interacting with a water molecule. As a consequence of its biradical nature the calculated $\langle S^2\rangle = 1.0$. The transition structure for concerted transfer of a hydroxyl radical to produce methanol, with hydrogen transfer to the NO_2 radical fragment forming H−ONO (TS-**10**), is just 5.2 kcal/mol higher in energy than MIN-**9**. This transition structure ($\langle S^2\rangle = 0.74$) is almost symmetrical with O···H distances between the NO_2 and the H_2O fragment of 2.092 and 2.095 Å and an O···C distance of 2.438 Å. An IRC calculation reveals that TS-**10** connects the $H_3C{\cdots}H_2O{\cdots}NO_2$ complex to the $CH_3OH{\cdots}HONO$ product complex (MIN-**11**). The first step along this pathway is C−O bond formation, and after the barrier is crossed an H transfer from the developing $CH_3-OH_2^+$ to the ONO fragment takes places leading to products, MIN-**11**. This final H-bonded product complex of methanol and HONO is 60.8 kcal/mol lower in energy than TS-**10**.

The oxidative process for the formation of methanol from HO−ONO and methane involves a number of intermediates that are weakly bonded. Consequently, the caveat must be included that in solution the actual process could resemble the one presented in Scheme 3. Solvent interactions could also potentially stabilize the intermediate complexes, and the solvent cage could involve diffusion of the intermediate radicals ($\cdot CH_3$, $\cdot NO_2$, $\cdot OH$). It is also possible that the water molecule that forms from HO−ONO in MIN-**9** and TS-**10** could be replaced by solvent water. However, all species involved are sufficiently short-lived with an activation barrier from MIN-**9** of only 5.2 kcal/mol that it is unlikely that diffusion could compete with a concerted collapse of MIN-**9** to product complex MIN-**11**. This is a highly exothermic oxidative process overall (−46.8 kcal/mol) that proceeds with a very low barrier once the metastable oxidizing reagent is formed. Additional evidence that the metastable form of peroxynitrous acid is involved in this hydrocarbon oxidation is the very large difference in activation energies for the unrestricted versus the closed-shell PES ($\Delta\Delta E^{\ddagger}$ = 15.7 kcal/mol) as shown by comparison of hydrogen abstraction transition structures TS-$\mathbf{6_R}$ and TS-**8** (Figure 7). These data strongly support involvement of the metastable form of peroxynitrous acid (HO−ONO*) advocated with tremendous insight by Pryor et al.[2,3] at the very outset of this rich new area of chemistry. These theoretical observations serve to corroborate the existence of a highly reactive reagent that has proven very difficult to pinpoint by experimental means.

(e) Oxidation of Isobutane with Metastable Peroxynitrous Acid.

$$\text{HO−ONO} + \text{isobutane} \rightarrow (CH_3)_3C{-}OH + \text{HONO} \quad (2)$$

We extended the study to the more realistic hydrocarbon substrate, isobutane, because this will involve a tertiary carbon center that can produce a much more stable tertiary radical center. It is for this reason tertiary carbon centers are typically attacked by open-shell reagents. The initial prereaction complex (MIN-**14**) between GS *cis*-HO−ONO and isobutane (Figure 9) is stabilized by only 0.2 kcal/mol with a distance between the oxygen atom of the peroxynitrous acid OH group and the hydrogen on the *tert*-carbon of 2.76 Å. The prereaction complex with *cis*-**2** is very weakly bound, and the TS for O−O bond elongation with the intramolecularly H-bonded *cis*-isomer is much more difficult to locate. Therefore, we used *trans*-**2** all along the reaction coordinate because it is lower in energy and because we found that it is much easier to locate the "excited" state intermediates on the reaction pathway. The TS for the O−O bond elongation process (TS-**15**) to form *trans*-HO−ONO*, in this case complexed with a molecule of isobutane (C···O distance 3.38 Å), is 10.0 kcal/mol higher than isolated cis reactants. The structure for O−O bond elongation for trans HO−ONO TS-**15** (complexed to isobutane) has an O−O bond distance of 1.871 Å and $\langle S^2\rangle = 0.38$. This TS, connecting to prereaction complex MIN-**16**, is almost identical with the TS for O−O bond breaking for trans HO−ONO itself (TS_{trans}-**2**). The O−O bond elongation TS leads to a complex (MIN-**16**) with an HO−ONO* fragment similar to that in the *trans*-**2** minimum albeit with *an isobutane molecule interacting with the OH group* (C···O distance 3.201 Å, O−O = 2.171 Å). The difference in energy between this minimum and the TS for O−O bond elongation (TS-**15**) is only 0.7 kcal mol^{-1}, and an $\langle S^2\rangle$ = 0.76 emphasizes its biradicaloid nature. MIN-**16** has a geometry poised for a facile H abstraction by the hydroxyl-like metastable reactant. The H abstraction TS (TS-**17**) is located only 0.3 kcal/mol higher than MIN-**16**. The geometry of this water producing TS is essentially that for H abstraction by OH radical complexed with an NO_2 radical. As noted above for the oxidation of methane, *the free OH radical is not involved* and the $\langle S^2\rangle$ = 0.86 for this structure is consistent with its open-shell character. Significantly, the pathway for this hydrogen abstraction step involving metastable *trans*-**2** has a lower activation barrier ($\Delta\Delta E^{\ddagger} = 5.9$ kcal/mol) than the concerted oxidation of isobutane involving TS-$\mathbf{15_R}$ on the RB3LYP PES (Figure 9). It is also noteworthy that the barrier for hydrogen abstraction from isobutane (TS-**17**, $\Delta E^{\ddagger} = 9.6$ kcal/mol) is considerably lower than that for the corresponding oxidation of methane (TS-**8**, $\Delta E^{\ddagger}$ = 15.4 kcal/mol) reflecting among other things the rather large difference in the C−H bond energies for isobutane and methane (G3, BDE = 96.7 and 104.1 kcal/mol, Table 2).

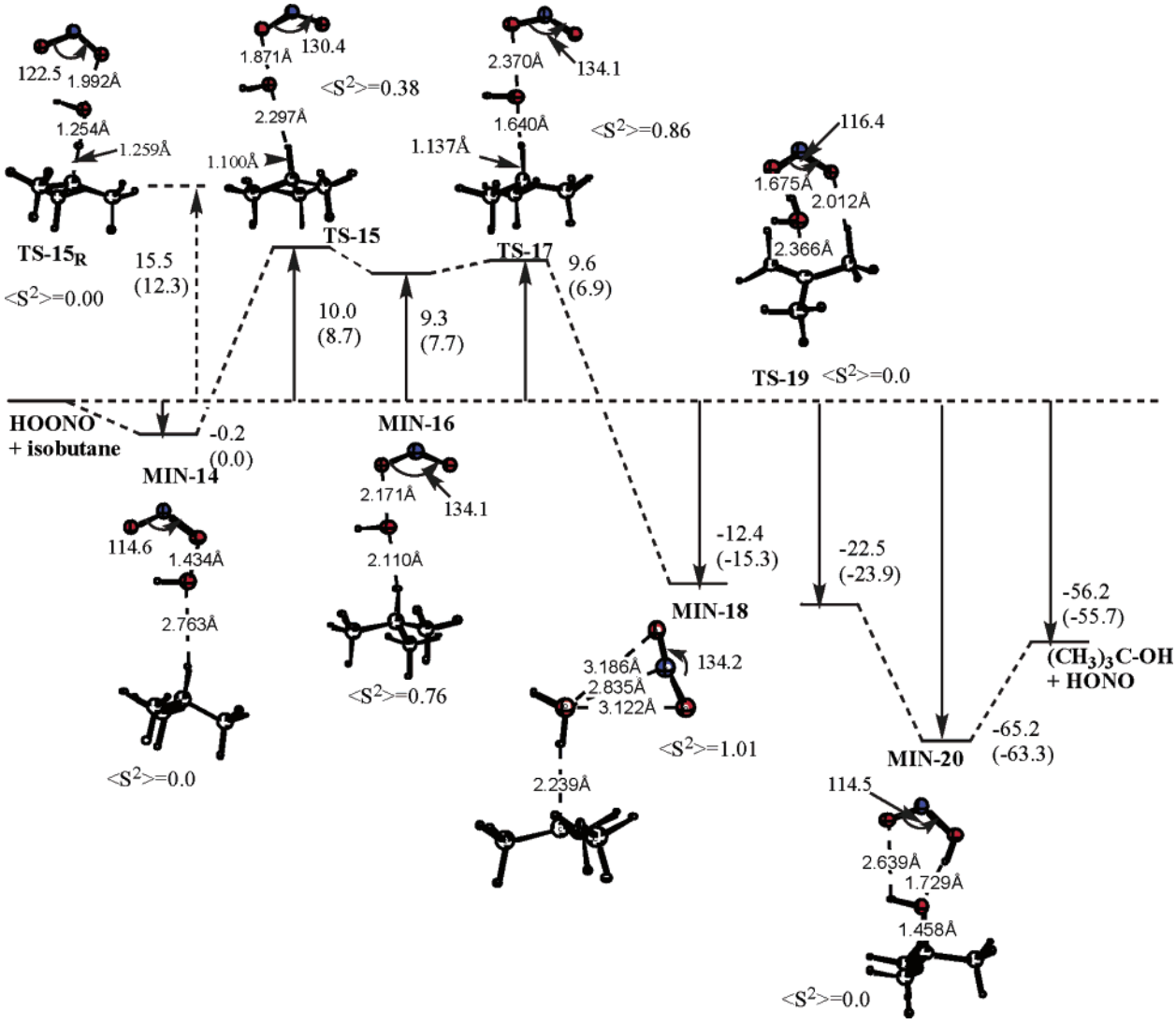

Figure 9. B3LYP/6-311+G(d,p) energy diagram for the HO−ONO oxidation of isobutane to *tert*-butyl alcohol. Relative energies in kcal/mol are with respect to isolated reactants (values in parentheses are with ZPE correction). [Prereaction complex of GS HO−ONO and isobutane, MIN-**14** (−439.433 09 au); transition structure for the abstraction of hydrogen from isobutane on the closed-shell surface, TS-**15**$_R$ (−439.408 04 au); Transition structure for O−O bond elongation in *trans*-**2** complexed to isobutane, TS-**15** (−439.416 87 au); MIN-**16** (−439.418 03 au); transition structure for hydrogen abstraction from isobutane on the unrestricted surface, TS-**17** (−439.417 56 au); MIN-**18** (−439.452 62 au); transition structure for the hydroxylation step, TS-**19** (−439.468 60 au); Product complex of *tert*-butyl alcohol and HONO, MIN-**20** (−439.536 67 au).]

Based upon the reaction vectors for TS-**17**, it is highly likely that this hydrogen abstraction reaction producing a water molecule is connected to MIN-**18**. This minimum structure can be described as NO_2 and $C(CH_3)_3$ radicals interacting with a water molecule. The O−H bond of the water molecule is weakly bonded to the carbon radical center at a distance of 2.24 Å. The ONO radical has retained its $^2A_1$ geometry with an ONO angle of 134.2°, and the diradicaloid complex has $\langle S^2 \rangle = 1.01$. However, the bonding interaction of an open-shell species such as a carbon radical with an oxygen atom containing a filled octet of electrons is bound to be extremely weak as exemplified by the interaction of dimethyl ether with a *tert*-butyl radical (**21,** Figure 10). The oxygen atom is not interacting with the carbon radical center but is weakly hydrogen bonded to an adjacent methyl group C−H with an essentially nonbonding binding energy (0.01kcal/mol). The same is true for the interaction of a water oxygen with the *tert*-butyl radical where the C···O distance is 4.3 Å and the complexation energy is only 0.15 kcal/mol (**22**, Figure 10). To achieve the hydroxylation step the water oxygen must be oriented toward the carbon radical. This requires that the water molecule in MIN-**18** must

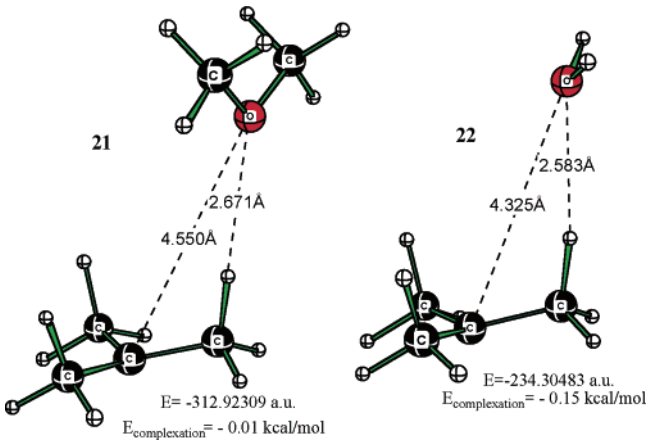

Figure 10. Complex of a *tert*-butyl radical with dimethyl ether (**21**) and with a water molecule (**22**) and optimized at the UB3LYP/6-311+G(d,p) level of theory. Complexation energies are calculated with ZPVE corrections.

rotate within the complex to achieve a more favorable geometry for forming the C−O bond of product *tert*-butyl alcohol. There is also the question of the extent of biradical character of the TS and whether this is the point at which the surface shifts from biradical to a pure singlet ($\langle S^2\rangle = 0.0$). The initial reactants and the final products of this overall oxidation scheme are obviously closed-shell species, so at some point along the overall reaction coordinate the open-shell character must revert to a ground-state closed-shell wave function with $\langle S^2\rangle = 0.0$.

We were able to locate a TS for this hydroxylation step (TS-**19**) that is 22.5 kcal/mol lower in energy than isolated reactants and also has $\langle S^2\rangle = 0.0$. It is noteworthy that the oxidation of methane (Figure 7) occurred completely on the open-shell surface until the final product complex (MIN-**11**). The surface for the oxidation of isobutane is distinctly different in that the latter half of the reaction pathway takes place on the closed-shell surface reflecting the greater stability of the tertiary carbon radical. Transition structure **19** has O···H distances between the NO_2 and the H_2O of 2.76 and 1.68 Å and an O···C distance of 2.37 Å. This hydroxylation TS is characterized by a low imaginary frequency (208.5i cm^{-1}) and finally leads to MIN-**20** which is the result of C−O bond formation with a H atom transfer from the developing $(CH_3)_3C-OH_2^+$ fragment to the ONO radical fragment presumably after the barrier is crossed. The reaction vector is comprised largely of an interaction of the hydrogen (0.38) and oxygen (0.42) of the transferring O−H group with the *tert*-butyl carbon center (C−O bond formation) and transfer of the H atom from the water molecule to the ONO fragment (0.31). The very relevant contraction of the ONO bond angle (116.4°) to its $^2B_2$ state was also represented in the reaction vector.

The difficulty in locating this particular gas-phase TS is a consequence of the fact that the attack of an open-shell *tert*-butyl free radical on the water molecule can occur from several directions, as determined by the spatial orientation of the oxygen lone pairs and must be accompanied by *the obligatory transfer of a hydrogen atom* to the ONO radical fragment. As noted above, the NO_2 radical, even in its higher energy $^2B_2$ state, does not readily engage in hydrogen abstraction from C−H bonds as noted by its high barrier (33.2 kcal/mol) for hydrogen abstraction (TS-**13**, Figure 8). In the absence of this complimentary H-transfer step, the water is weakly bound to the *tert*-butyl radical at a distance far too great (4.3 Å) to achieve C−O bond formation (**22**, Figure 10). The exact balance of this nonsynchronous but concerted process must be maintained in the reaction vector in order to even get close to the correct transition structure. As noted above TS-**19** has a low imaginary frequency (208.5i cm^{-1}) characteristic of the heavy atom motion attending C−O bond formation with H atom transfer from the $(CH_3)_3C-OH_2^+$ fragment to the ONO radical presumably after the barrier is crossed finally leading to MIN-**20**. It is highly unlikely that a hydrogen atom is first transferred from water to the ONO radical due to a very large disparity in the O−H bond energies involved. The O−H BDE of H−ONO is 77.6 kcal/mol (Table 2) in contrast to the strong O−H BDE of water (G3, 118.0 kcal/mol). The O−H bond in H−ONO is much weaker than that in either *cis*-ONO−O−H (87.3 kcal/mol) or nitric acid (106.3 kcal/mol). These data argue strongly for a concerted hydroxylation step with hydrogen transfer to the $^2B_2$ NO_2 radical late along the reaction coordinate. This final H bonded structure (MIN-**20**) is a closed-shell singlet ($\langle S^2\rangle = 0.0$) and is 65.2 kcal/mol more stable than isolated HO−ONO and isobutane. The overall oxidation process is exothermic by −56.2 kcal/mol (Figure 9).

The overall reaction surface for HO−ONO* isobutane oxidation does have one problem that remains to be resolved. The TS for O−O bond elongation (TS-**15)**, the prereaction complex MIN-**14**, the TS for hydrogen abstraction (TS-**17**), and MIN-**18** all have open-shell character suggesting that the oxidation of isobutane involves two steps, but not necessarily involving a discrete long-lived biradicaloid intermediate on the entire reaction pathway. The hydrogen abstraction TS (TS-**17)** is indeed a diradical ($\langle S^2\rangle = 0.86$) with very little charge separation. The *tert*-butyl radical fragment has a calculated charge of −0.057 electrons, while the sum of the ONO radical (0.021 e) and the water molecule has a charge of 0.057e.

The second part of the reaction surface constitutes the hydroxylation step (TS-**19**) that is connected to the *tert*-butyl alcohol HONO complex on the product side (MIN-**20**). Both the TS and products are closed-shell in nature ($\langle S^2\rangle = 0.0$). However, we had difficulty in identifying a singlet minimum on the reactant side of TS-**19**. While TS-**19** may formally be considered to be a diradical, examination of the charges on the three fragments show that the $^2B_2$ NO_2 fragment (ONO angle of 116.4°) has a charge of −0.697 while the charge on the *tert*-butyl fragment is actually positive (+0.584) exhibiting carbonium ion character. Consequently, this charge-separated ionic complex is not actually biradicloid in nature and has an $\langle S^2\rangle = 0.0$. All attempts to locate the minimum connected to this singlet on the reactant side of TS-**19** resulted in an elimination pathway affording isobutene. A series of putative intermediates potentially connected to TS-**19** on the reactant side of the reaction surface all had total energies that were essentially identical. An IRC calculation shows that TS-**19** is, as anticipated, connected to the products *tert*-butyl alcohol, but surprisingly it is also connected to the elimination surface leading to isobutene (Figure 11, MIN-**23**). This behavior is reminiscent of the bifurcation point behavior suggested earlier by Rauk and co-workers for the dioxirane oxidation of hydrocarbons.[7e] Although this second potential pathway for HO−ONO* oxidation of isobutane involves the formation of isobutene, the primary oxidative pathway for the HO−ONO* oxidation of isobutane to *tert*-butyl alcohol is more exothermic [$\Delta\Delta E = 12.4$ kcal/mol, Figure 11) than the secondary pathway leading to isobutylene (eq 3).

$$\text{HO}-\text{ONO} + \text{isobutane} \rightarrow (CH_3)_2C{=}CH_2 + H_2O + \text{H}-\text{ONO} \quad (3)$$

Our search for the reactant minimum connected to TS-**19** proved quite difficult. We were surprised initially to observe a facile abstraction of a hydrogen atom from the *tert*-butyl radical by the ONO fragment. This is all the more confusing when you observe that the ONO radical is actually a rather feeble reagent for H abstraction when compared to the OH radical ($\Delta\Delta E^{\ddagger} = 30.9$ kcal/mol, Figure 8). However, it is the very weak α-C−H bond of the methyl group (BDE = 38.3 kcal/mol) adjacent to the carbon radical center in *tert*-butyl radical in developing MIN-**23** that determines the overall pathway (Table 2).

(f) Oxidation of Dimethyl Sulfide and Dimethylselenide. It now remains to resolve the issue of HO−ONO attack on closed-shell systems with a filled octet of electrons. The attack

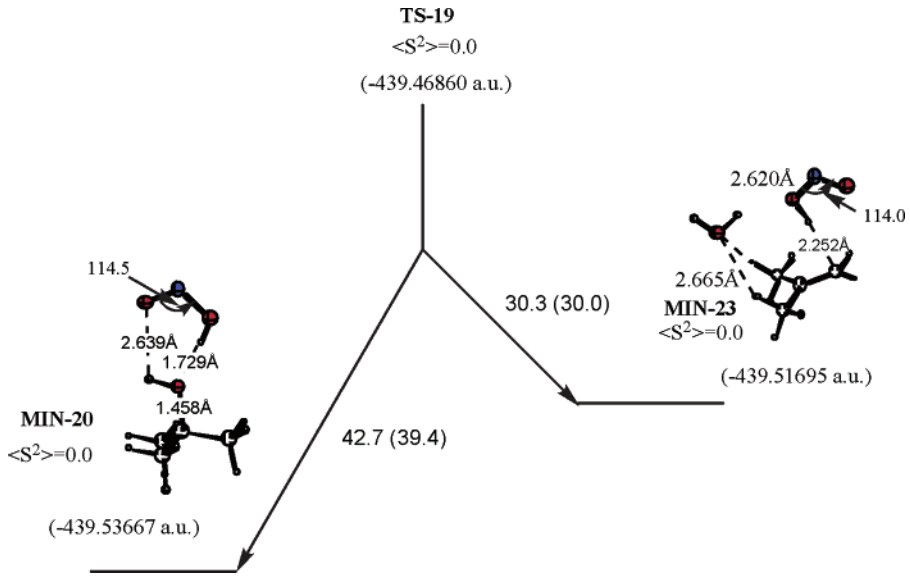

Figure 11. Potential bifurcation point showing TS-19 leading to both the anticipated *tert*-butyl alcohol product (MIN-**20**) and elimination from the *tert*-butyl fragment to form water and isobutylene (MIN-**23**). The IRC was carried out at the B3LYP/6-311+G(d,p) level. Relative energies in kcal/mol are with respect to isolated reactants (values in parentheses are with ZPE correction).

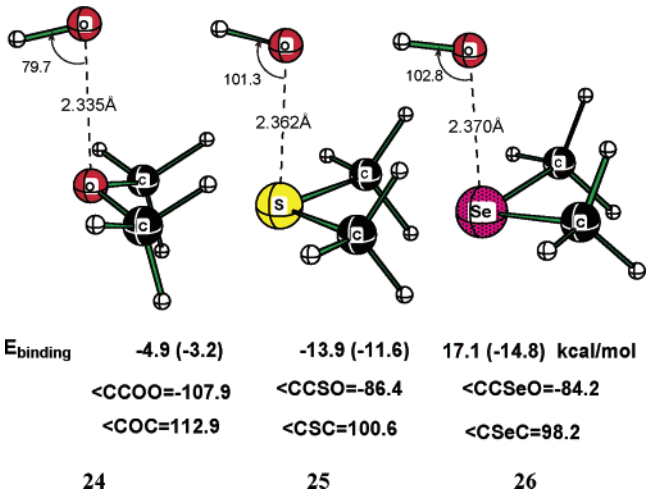

Figure 12. OH radical adducts of CH_3OCH_3 (**24**), CH_3SCH_3 (**25**), and CH_3SeCH_3 (**26**) optimized at the UB3LYP/6-311+G(d,p) level of theory. Energy of binding ($E_{binding}$) is based upon total UB3LYP/6-311+G(d,p) energies of the adducts, OH radical, and DMS/DMSe. Numbers in parentheses are calculated with the ZPVE corrections.

of an open-shell species on a second or third row element can in principle proceed by expansion of the octet of electrons. A comparison of the minima resulting from addition of hydroxyl radical to O, S, and Se atoms is demonstrated in Figure 12 (**24**, **25**, and **26**). While the bonding distance of the OH radical to the heteroatoms of dimethyl ether dimethyl sulfide (DMS) and dimethyl selenide (DMSe) remains surprisingly constant at 2.3 Å, the binding energy increases with the size of the heteroatom.

Thus, it would appear quite feasible that HO−ONO could react with such two-electron substrates quite readily on the free radical pathway (Scheme 1). This problem has been thoroughly examined by Museav et al.,[15b] and it was concluded, on the basis of relative energetics, that in the gas phase a stepwise pathway (one-electron oxidation) involving O−O bond homolysis followed by coordination with DMS is the lower energy path.

Our primary objective was to search for an unrestricted or open-shell PES for oxidation of DMS and DMSe. Ground-state HO−ONO does form a prereaction complex with DMS with a stabilization energy of −2.85 kcal/mol relative to isolated reactants DMS and HO−ONO **(27a**, Figure 13).

In this loosely bound complex the S−O and O−O distances are 3.085 and 1.445 Å. However, the "excited state" of HO−ONO also forms loosely bound complex **27b** with DMS with S−O and O−O distances of 2.31 and 2.66 Å that is only 1.7 kcal/mol higher in energy despite the larger energy difference between *cis*-GS HO−ONO and *cis*-**2** (12.2 kcal/mol, Figure 1). These data are suggestive of a possible oxidation involving hydroxylation of DMS with a hydrogen transfer producing the H−ONO fragment later along the reaction pathway much in the same fashion as peracid oxidation.

However, despite repeated attempts on the unrestricted surface (UB3LYP) with an initial $\langle S^2\rangle = 1.0$, we always arrived at the transition structure with an $\langle S^2\rangle = 0.0$ on the closed-shell restricted surface. The relatively short O−O distances in TS-**28** and TS-**29** (Figure 13) are also quite indicative of a two-electron oxygen transfer reaction as we described previously.[8a] We are left with the conclusion that the oxidation of such two-electron nucleophiles as DMS and DMSe follow the pathway originally suggested, an S_N2-like attack of the heteroatom lone pair on the σ^* O−O orbital of GS HO−ONO.

Conclusion

(1) Both cis and trans forms of metastable isomers of peroxynitrous acid with elongated O−O bonds have been found and verified at several levels of theory including QCISD, BD-(TQ), and CASSCF. Metastable isomers *cis*-**2** and *trans*-**2** are only 14.4 (8.2) and 13.2 (7.2) kcal/mol higher in energy than ground state cis HO−ONO at the UB3LYP and spin-corrected UB3LYP (in parentheses) levels. This is in excellent agreement with the MRCI values of 11.7 and 9.0 kcal/mol for *cis*-**2** and *trans*-**2** with respect to *perp*-HO−ONO ground state.

(2) Transition structures for O−O bond elongation of both cis and trans ground-state HO−ONO have been located [$\langle S^2\rangle = 0.52$ and 0.43 at the UB3LYP/6-311+G(3df,2p) level], and we suggest that both TS_{cis}-**1** and TS_{trans}-**2** are connected to the metastable isomers *cis*-**2** and *trans*-**2** retaining a weak contribution from the O−O bond (HO····ONO).

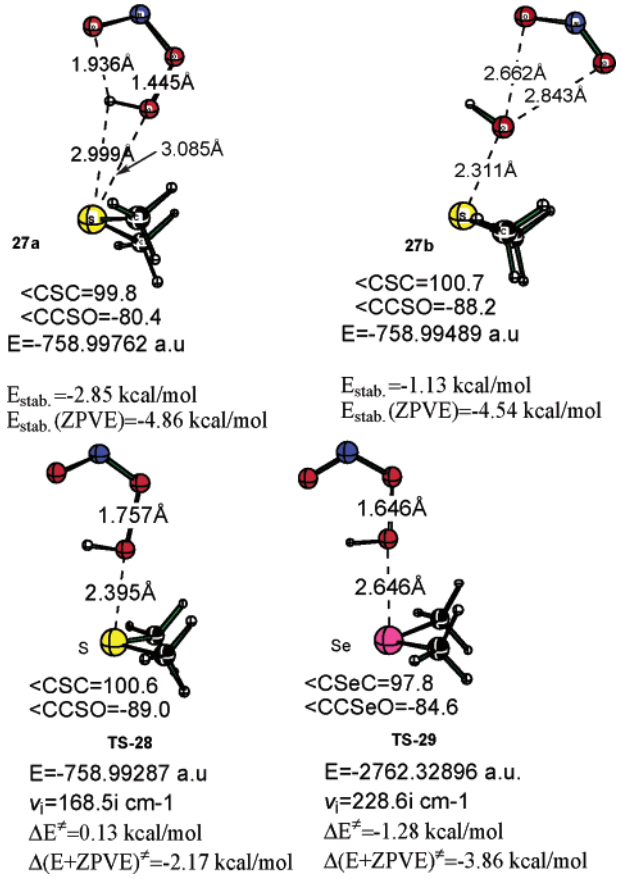

Figure 13. UB3LYP/6-311+G(d,p)-optimized complexes of *cis*-GS HO−ONO and metastable *trans*-**2** with DMS [**27a** ($\langle S^2\rangle = 0.0$) and **27b** ($\langle S^2\rangle = 0.9$)] and two transition structures for the reaction of HO−ONO with DMS (TS-**28**) and DMSe (TS-**29**) optimized at the RB3LYP/6-311+G(d,p) level of theory. The complexation energy (E_{stab}) and the activation barriers [$\Delta E^{\ddagger}$ and $\Delta(E+ZPVE)^{\ddagger}$] are calculated with respect to isolated reactants [DMS (−478.066 69 au), DMSe (−2481.400 54 au), and HOONO *cis*−*cis* (−280.926 38 au)].

(3) Geometry optimization of both *cis*-**2** and *trans*-**2** within the COSMO solvent model suggest that both could exist as energy minima in polar media. Specifically solvated forms of metastable *cis*-**2** and *trans*-**2**, hydrogen bonded to three molecules of water (*cis*-**2**·$3H_2O$ and *trans*-**2**·$3H_2O$), are stable minima only 12 kcal/mol higher in energy than solvated ground-state HO−ONO. We suggest that these types of solvated metastable forms of peroxynitrous acid represent the elusive higher lying biradicaloid minima (HO−ONO*) described previously in the experimental literature.

(4) Isomeric forms of *cis*-**2** and *trans*-**2** (**4A** and **4B**) with the hydroxyl radical weakly hydrogen bonded to the ONO radical fragment (•OH····ONO•) are slightly higher in energy than metastable *cis*-**2** and *trans*-**2** at the UQCISD/6-311+G-(d,p)//UQCISD/6-311+G(d,p) level (Table 1) but slightly lower in energy with a G3B3 energy correction when the geometries are optimized at the B3LYP/6-311+G(3df,2p) level. The energy difference does widen to 6−9 kcal/mol when the Yamaguchi correction to the spin-contamination is included. However, isomeric **4A** and **4B** have weak hydrogen bonds between the hydroxyl radical and the ONO radical fragment (1.1 kcal/mol) and do not appear to be stable in aqueous solution.[15] However, in a hydrophobic environment both forms of these higher lying singlet of peroxynitrous acid could potentially serve as a latent source of *weakly bound* hydroxyl radical.

(5) Isomerization of peroxynitrous acid to nitric acid does not involve a concerted 1,2-OH shift but rather involves prior O−O bond dissociation and recombination.

(6) The potential energy surface for the HO−ONO oxidation of methane to methanol takes place on the unrestricted or open-shell surface and involves metastable *trans*-**2**. The transition state for the O−O bond elongation of HO−ONO, complexed to a molecule of methane, produces a prereaction complex (**MIN-7**, Figure 7) in which the HO−ONO fragment is essentially identical to metastable *trans*-**2** maintaining a weak but discernible O−O bond. The transition state for hydrogen abstraction from methane (**TS-8**, Figure 7) involving the metastable form of HO−ONO is 15.7 kcal/mol lower than the corresponding hydrogen abstraction on the closed-shell surface (**TS-6$_R$**, $\Delta E^{\ddagger} = 31.1$ kcal/mol). The activation barrier for hydrogen abstraction from methane by a free hydroxyl radical is only 2.3 kcal/mol (Figure 8).

(7) Peroxynitrous acid oxidation of isobutane also involves metastable *trans*-**2** hydrogen bonded to isobutane (**MIN-16**, Figure 9). The hydrogen abstraction step (**TS-17**) has an activation energy of 9.6 kcal/mol relative to isolated reactants GS HO−ONO and isobutane but only 0.3 kcal/mol relative to its prereaction complex **MIN-16**. Significantly, the metastable form of HO−ONO, *trans*-**2**, is readily identifiable in the transition structure for hydrogen abstraction having an O−O bond distance of 2.37 Å and an ONO angle of 134.1°. This hydrogen abstraction TS on the unrestricted surface (**TS-17**) is 5.9 kcal/mol lower in energy than the corresponding closed-shell or restricted potential energy surface (**TS-15$_R$**, $\Delta E^{\ddagger} = 15.5$ kcal/mol). These combined data corroborate earlier suggestions[3] that some form of activated or excited peroxynitrous acid (HO−ONO*) could be involved in biochemical processes.

(8) The overall hydrocarbon oxidation process involving metastable forms of peroxynitrous acid is very likely a concerted but nonsynchronous reaction, since the hydroxylation step (**TS-19**) involving attack of a water molecule on a putative *tert*-butyl radical cannot readily take place in the absence of the obligatory transfer of a hydrogen atom from water to the developing $^2B_2$ ONO radical. The reaction of the closed-shell oxygen atom of a water molecule with a carbon radical center is extremely weak (Figure 10).

(9) While metastable *cis*-**2** can form a weak complex with a two-electron nucleophile like dimethyl sulfide or dimethyl selenide (Figure 12), the oxygen atom transfer step to produce the heteroatom oxide takes place on the closed-shell or restricted surface.

Acknowledgment. This work was supported by the National Science Foundation (CHE-0138632) and partially supported by the National Computational Science Alliance under CHE990021N and utilized the NCSA SGI Origin2000 and University of Kentucky HP Superdome.

Supporting Information Available: Total energies, Cartesian coordinates, and CASSCF orbitals. This material is available free of charge via the Internet at http://pubs.acs.org.

JA044245D